



# ***Bauhinia variegata* Bark Extract: Assessment of its Anti-proliferative and Apoptotic Activities on A549 and H460 Lung Cancer Cell Lines**

**Tanvi Khanna, Akash Dave, Sejal Purani, Jagath Vedamurthy, Dhaval Jivani and Pushpa Robin\***

Department of Biochemistry, The Maharaja Sayajirao University of Baroda, Vadodara - 390002, Gujarat, India; pushparobin@gmail.com

## **Abstract**

The hunt for novel anticancer drugs with minimal side effects continues. This study strengthens the claim by providing biochemical evidences of anticancer activities of *Bauhinia variegata* bark extracts on lung carcinoma cells (A549 and H460). Bark extracts of *Bauhinia variegata* were prepared by different solvents using Soxhlet apparatus and tested for their antioxidant potential by DPPH assay. The lung cancer cell lines were treated with *Bauhinia variegata* bark extracts and viability of cells was measured by MTT assay; metastatic ability was determined through Scratch assay and effect on DNA integrity was shown by gel electrophoresis. The Petroleum Ether Bark Extract (PEBE) inhibits proliferation (A549, IC50 = 1.5 mg/ml) at 48 h treatment. DNA damage was observed in A549 cells by agarose gel electrophoresis. The Chloroform Bark Extract (CBE) inhibited proliferation of H460 (IC50 = 1 mg/ml) with DNA damage after 24 h treatment. Soft agar assay indicated decreased ability to form colonies and scratch test showed impaired migration of A549 and H460 to PEBE and CBE treatment respectively. Apoptosis was detected using fluorescent dye staining in A549 and H460 cells. Caspase 3 activity was increased significantly in A549 and H460 cells. PEBE and CBE decrease the mitochondrial membrane potential gradient ( $\Delta\Psi_m$ ) of A549 and H460 cells respectively. This study categorically proves the cytotoxic activity of *Bauhinia variegata* bark extracts on A549 and H460 cells.

**Keywords:** Anticancer Effect, Caspase, DNA Damage, Metastasis, Non-small Cell Lung Cancer Cell Lines

**Abbreviations:** Non-Small Cell Lung Cancer (NSCLC), 3-(4,5-Dimethylthiazol-2-yl)-2,5-diphenyltetrazolium bromide (MTT), Petroleum Ether Bark Extract (PEBE), Chloroform Bark Extract (CBE), Petroleum Ether (PE), N-hexane (HX), Chloroform (CHL), Ethyl Acetate (EA), Methanol (MET), Water (AQ), Dimethyl sulfoxide (DMSO), 2, 2-Diphenyl-1-picrylhydrazyl (DPPH), Standard Deviation (SD), Standard Error of Mean (SEM), Dulbecco's Modified Eagle's Medium (DMEM), 2',7'-dichlorodihydrofluorescein diacetate (H2DCF-DA), Phosphate Buffer Saline (PBS), Hydrogen peroxide (H2O2), TAE (Triacetate- EDTA), Sodium Chloride (NaCl), Half Maximal Inhibitory Concentration (IC50), Tetramethyl Rhodamine, Methyl Ester (TMRM),

4',6-diamidino-2-phenylindole (DAPI), Analysis Of Variance (ANOVA), Acridine Orange (AO), Ethidium bromide (EtBr)

## **1. Introduction**

Exponential increase in cancer incidences is a global burden. Every year India reports about 70,275 lung cancer cases (fourth among all cancers) with 50 % mortality within a year and 5-year survival has remained at 11-17 % for these lung cancer patients<sup>1,2</sup>. Non-small cell lung cancer (NSCLC) contributes for about 85 % of the lung cancer cases while 15 % cases are SCLC<sup>2</sup>.

\*Author for correspondence

The most typical NSCLC is adenocarcinoma (40 %), followed by large cell carcinoma (15 %)³. Hence, in this study A549 (adenocarcinoma) and H460 (large cell carcinoma) cell lines were used. The 5-year relative survival rate of lung cancer has increased with time, but less than 21 %³. The poor survival rate along with low efficacy and side effects of chemotherapy (20-30 %) are major causes of concern in lung cancer⁴,⁵. The side effects related to present drugs motivates scientists to search for anticancer compounds from natural sources such as plant phytochemicals. Phytochemicals have lower toxicity providing an attractive alternative in cancer therapy⁶,⁷. Plant of our interest is *Bauhinia variegata*, a species in the legume family, Fabaceae. It is commonly known as Mountain Ebony, which is a medium-sized deciduous tree found throughout India. *Bauhinia variegata* L. has been mentioned in traditional texts to have multiple pharmacological activities⁸ with preliminary proof of *in-vitro* cytotoxic activity of leaf and bark extracts. Government of India has given a lot of emphasis on bringing its traditional ayurvedic knowledge to greater acceptability through validation using biochemical mechanisms involved⁹.

Cancer cells has increased ROS levels as compared to their normal counterparts and are detoxified by complex antioxidative mechanisms¹¹. Progression of cancer has been shown to follow changes in ROS¹⁰-¹². A fall out in Oxidative stress happens due to imbalance between the systems which generates and scavenges ROS. Cell apoptosis progresses with distinct biochemical pathways and plays a critical role in development and homeostasis¹³. Cancer cells have the ability to circumvent apoptosis making proteins involved in the apoptotic cascades as ideal targets for cancer therapy¹⁶. Reestablishing apoptotic programming in malignant cells selectively kills tumor cells and caspases as primary inducers of apoptosis provide an ideal platform to develop effective therapeutic strategies for cancer¹⁴,¹⁵. Here, we report the biochemical basis for the effective anticancer potential of *Bauhinia variegata* bark extracts on lung cancer.

## 2. Material and Methods

### 2.1 Plant Material Collection and Phytoextraction

*Bauhinia variegata* bark was collected from Waghai botanical garden, Dang, Gujarat during December-January each year and was validated by the Department of Botany, The Maharaja Sayajirao University of Baroda, India. The bark was washed, surface sterilized with 0.1 % mercuric chloride, rinsed - shade dried, powdered and packed into a thimble for extraction by Soxhlet method with eluotropic series for 8-12 hr¹⁶. The dry sample was dissolved in DMSO to form a 100 mg/ml stock & filtered by a 0.22 µm syringe filter for further use.

### 2.2 Qualitative Analysis of Phytoextracts

Qualitative analysis (alkaloids, fatty acids, cardiac glycosides, flavonoids, glycosides, phenols, resins, saponins, steroids, tannins, terpenoids) of *Bauhinia variegata* bark extracts was done using standard procedures¹⁷,¹⁸.

### 2.3 Determination of Antioxidant Activity by DPPH Assay

The antioxidant activity was measured using DPPH free radical assay by a standard protocol¹⁷.

### 2.4 In Vitro Culturing of Human Lung Cancer Cell Lines

Human lung cancer cell lines A549 and H460 were obtained from (NCCS, Pune, India). Cell lines were grown as per the standard protocol in controlled environment and supplements¹⁹.

### 2.5 MTT Method (Cytotoxic Assay)

The stock solutions of *Bauhinia variegata* bark extracts were prepared in 0.5 % Dimethyl Sulfoxide (DMSO) and diluted for further use (DMSO concentration

did not exceed 0.1 %). Cytotoxic potential of extract was determined by MTT assay<sup>19</sup>. Cells were grown in 96-well plates overnight and treated with different concentrations of bark extracts for 24 h, 48 h and 72 h time points. Untreated cells were taken as control. After 24, 48 and 72 h of incubation of cell lines with bark extracts, MTT assay was done using standard protocols<sup>19</sup>. The absorbance of each well was measured at 575 nm. IC50 value of extracts was calculated by determining percentage cell growth inhibition using Graph Pad Prism 6.0 software.

## 2.6 Soft Agar Colony Formation to Evaluate Cellular Transformation

For Colonogenic assay, the cells were plated in 6-well tissue culture plate with 5,000 viable cells (per well) as determined by the Trypan blue staining<sup>20</sup>. A549 and H460 cells were allowed to grow overnight and after 24 h the fresh media modified with different concentrations of the different extracts were added for 48 h and 24 h respectively. The number of A549 and H460 cells after treatment with respective extracts were counted using a Neubauer Chamber. 2 % Agar was melted and cooled to 40°C in a water bath and media containing serum was added in equal volume to give 1 % base agar solution. 500µl of the base agar solution was pipetted into each well of a 24-well plate. 0.7 % agar was melted and cooled to 40 °C and mixed with media containing A549 cells treated with PEBE for 48 h.

For H460, 0.7 % agar was mixed with media containing H460 cells treated with CBE for 24 h. 500µl of this solution was pipetted onto the top agar. Cell number was maintained at 1250-1500 cells per well. The cells could grow for 13 -15 days for both cell line and in every 3-4 days, 200 µl of fresh media was added above the top layer as a feeder. After 15 days, the medium above the cells was removed and rinsed carefully with PBS. 2-3 ml of a mix of 6.0 % glutaraldehyde and 0.5 % crystal violet was added on cells and left for a minimum 20 min. The glutaraldehyde crystal violet mixture was removed and rinsed with water. The colony size was measured using Image J software.

## 2.7 Wound Healing Assay/Scratch Test

Cancer cells undergo epithelial to mesenchymal transition during metastasis<sup>21,22</sup>. Cells were grown

and starved in low serum media (1.5 ml; 2 % serum in DMEM) overnight. A549 and H460 cells monolayers were scraped during a line to make a “scratch” with a pipette 200 µl tip. Cells were washed with PBS and low-serum media (2 % serum to prevent cell proliferation) was replaced with media containing different concentrations of extracts. A549 cells were treated with PEBE extract for 48 h and H460 cells with CBE for 24 h. Plates were placed in an incubator at 37 °C for 0-36 h. Cells were stained with crystal violet and images were captured at different time-points from 0 to 36 h respectively. The pictures acquired for every sample was further analyzed quantitatively by using computing software.

## 2.8 DNA Fragmentation Examination

A549 and H460 cells ( $5 \times 10^6$ ) were grown for 24 h and treated with various concentrations of PEBE and CBE for 48 h and 24 h, respectively. Cells were collected, washed with  $1 \times$  PBS and centrifuged at 300 g. Cell pellet was collected and resuspended in 0.5 ml lysis buffer and incubated for 1.5 h at 37 °C followed by centrifugation at 10 K rpm for 15 min (at room temperature). Pellet was discarded and supernatant was mixed with equal volume of isopropanol followed by an addition of 25 µl of 4M NaCl and incubated at -20 °C overnight. Mixture was centrifuged again at 10 K rpm for 20 min and the pellet was dissolved in 40 µl ddH<sub>2</sub>O. 5 µl of RNase A (10 mg/ml) was added to the lysate and further incubated for 1 h at 37 °C. The DNA was then electrophoresed in a 1.8% agarose gel in TAE (triacetate-EDTA) buffer (pH 8.0). After electrophoresis, ethidium bromide was used to stain the DNA and visualized using a gel-doc system (BIO-RAD).

## 2.9 Analysis of Intracellular Reactive Oxygen Species by DCHF-DA

The 2', 7'-dichlorodihydrofluorescein diacetate (H2DCF-DA) fluorescent probe is commonly employed that enabled the monitoring of intracellular accumulation of ROS. A549 and H460 cells were grown overnight in 6 well plates. Cells were treated with PEBE (A549) and CBE (H460) respectively and incubated for various time intervals (0 to 10h). At the end of the incubation period, the media was removed and 5 µM of DCHF-DA which is diluted in media was added to

the cells and incubated for 40 min at 37 °C. Remove the dye, trypsinize the cells and add media to stop its action. Centrifuge it at 1500 rpm for 3 min. The cells were then washed thrice with PBS and fluorescence intensity (excitation = 485 nm and emission = 530 nm) was measured by fluorimeter<sup>7,23</sup>.

## 2.10 Fluorescent Microscopy Analysis by DAPI Staining and Acridine Orange/Ethidium Bromide Staining

Cell nuclear morphology was checked by fluorescence microscopy using DAPI<sup>24</sup> and AO/EtBr staining<sup>16,25</sup>. A549 cells were treated with the PEBE for 48 h and H460 cells with CBE for 24 h followed by DAPI and AO/EB dye mix and examined under a Nikon Eclipse Ti fluorescence microscope.

## 2.11 Determination of Caspase-3 Activity in Cell Lines

Bio Vision Caspase-3 Colorimetric assay kit (K-106) was used to determine caspase-3 levels in A549 and H460 cell lines as per the protocol mentioned in the kit instruction manual.

## 2.12 TMRM Staining for Mitochondrial Membrane Potential Measurement

A549 and H460 cells were grown in 6-well plates and treated with PEBE (IC<sub>50</sub>, 48 h) and CBE (IC<sub>50</sub>, 24 h) respectively. The cells were stained with tetramethyl rhodamine, methyl ester and perchlorate (TMRM, 100 nM) at 37 °C for 30 minutes<sup>25,26</sup>. After PBS wash, the cells were imaged using a fluorescence microscope.

## 2.13 Statistical Analysis

All experiments were done in triplicate, and data expressed as mean ± standard error of mean (SEM).

# 3. Results

## 3.1 Extract Preparation and Determination of Antioxidant Potential

*Bauhinia variegata* bark was ground after washing and drying, the powder so obtained was weighed and

subjected to solvent extraction by Soxhlet apparatus. Various fractions of crude extracts were collected and tested for their effects on A549 and H460 cell lines. The classes of phytochemicals present in these extracts were identified to be oils and fats, alkaloids, carbohydrates, saponin and glycosides in PEBE (while phenols, flavonoids and triterpenoids were absent and the CBE contained phytochemicals like (oils and fats, alkaloids, saponin, polyphenols, cardiac glycoside, tannin, and terpenoids (Data not shown here). GC-MS chromatogram of the PEBE of *Bauhinia variegata* clearly showed the presence of 18 compounds and GC-MS chromatogram of the CBE of *Bauhinia variegata* clearly showed the presence of 08 compounds (Data not shown here).

Further, the antioxidant potential of the extracts was determined by DPPH assay which showed that n-hexane and petroleum ether extracts showed lesser antioxidant activity as compared to other extracts. The methanolic and water extracts showed maximum antioxidant activity with the strongest DPPH radical scavenging activity among all the extracts (Figure 1). Percentage scavenging of DPPH free radical with different concentrations of *Bauhinia variegata* bark extracts here.

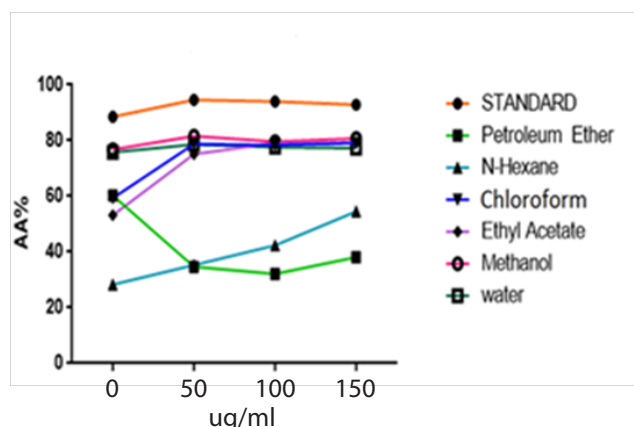


**Figure 1.** Percentage scavenging of DPPH free radical with different concentrations of *Bauhinia variegata* bark extracts.

## 3.2 MTT Assay: Potential for Cytotoxicity

### 3.2.1 Cytotoxic Screening of Extracts on A549 Cells by MTT Assay

The effect of the various extracts was evaluated on A549 cell line. Cytotoxic activities against A549 cells growth

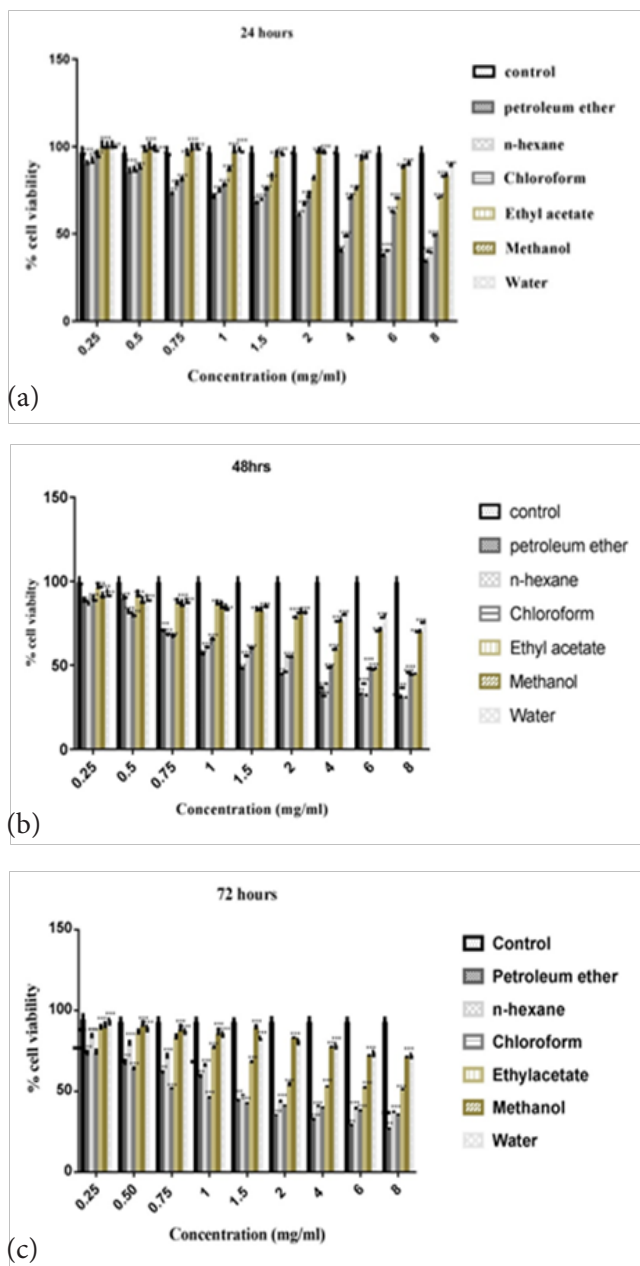


**Figure 2.** The effect of *Bauhinia variegata* bark extracts against A549 cell line for 24 h, 48 h and 72 h. Percentage growth proliferation of A549 cells was assayed at 100 mg/ml concentration of extracts using MTT assay as described in the Methods section (a) Effect of different concentrations of different bark extracts on A549 cells for 24 h (b) Effect of different concentrations of different bark extracts on A549 cells for 48 h (c) Effect of different concentrations of different bark extracts on A549 cells for 72 h respectively. Data represented as the mean  $\pm$  standard deviation of at least three experiments. \*\*\* $P < 0.001$ .

were measured after treating with phytochemical extracts of PE, N-hexane, Chloroform, Ethyl acetate, Methanol and Water of *Bauhinia variegata* at concentrations of 0.25 mg/ml to 8mg/ml for 24 h, 48 h and 72 h. The results showed that A549 cells responded to the cytotoxic effects of the plant extracts in a dose and time-dependent manner.

Petroleum ether and n-Hexane extracts showed the foremost cytotoxic effect on A549 cell line as compared to other extracts at 48 h treatment. The polarities of Petroleum ether and n-hexane are almost similar and both the solvents have shown almost similar composition. Hence, it's likely that the cytotoxic agent (s) in both the solvents are identical. Therefore, Petroleum ether bark extract (PEBE) has been selected for the further study due to lesser yield of n-hexane extract. The cytotoxicity of PEBE on A549 cells increased from 33 % to 30 % to 26 % after 24, 48 and 72 h respectively. The cytotoxicity of PEBE on A549 cells is shown in Figure 2 a, b, c.

### 3.2.2 PEBE Inhibit Growth and Proliferation of A549 Cells

Examination of A549 cell morphology was done at 48 h treatment of PEBE and it was observed that from 0.5, 1, 1.5, 2 and 4 mg/ml concentrations cells had altered morphologically and started to shrink showing the symptoms of the cell death. The morphological examination of the cells after PEBE treatment showed cell shrinkage and rounding up of the cells which are typical features of cell death as shown in Figure 3.

### 3.2.3 Determination of IC<sub>50</sub> Value of PEBE Extract

Effect of different concentrations of PEBE of *Bauhinia variegata* on the viability of A549 cells for different time measure (at 24 h, 48 h and 72 h) was assessed. The IC<sub>50</sub> values were 2.8 mg/ml for 24 h, 1.6 mg/ml for 48 h and 1.5 mg/ml for 72 h as shown in Figure 4. The extract was more potent after 48 h treatment; hence this time point was selected for further experiments (Figure 4).

## 3.3 MTT Assay - H460 Cells

### 3.3.1 Cytotoxic Screening of Extracts on H460 Cells

The effect of the extracts on H460 cell line showed that the chloroform bark extract (CBE) had a greater

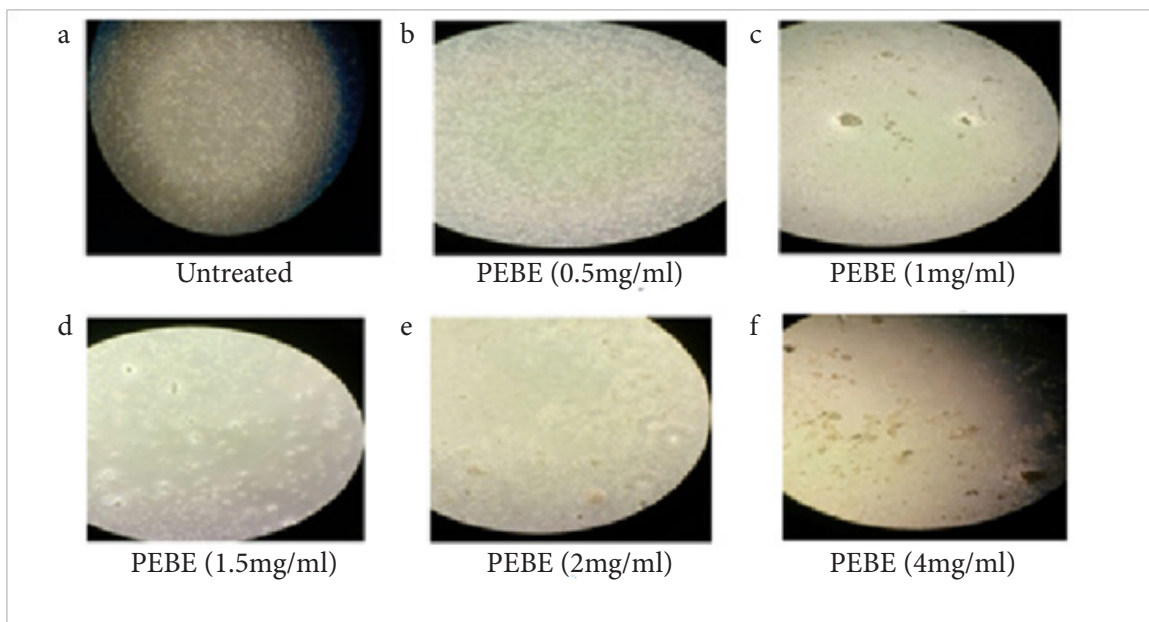


**Figure 3.** Morphological effects of A549 untreated cells (a) without treatment and cells exposed to (b) PEBE (0.5 mg/ml), (c) PEBE (1 mg/ml), (d) PEBE (1.5 mg/ml), (e) PEBE (2 mg/ml), (f) PEBE (4 mg/ml) of *Bauhinia variegata*.

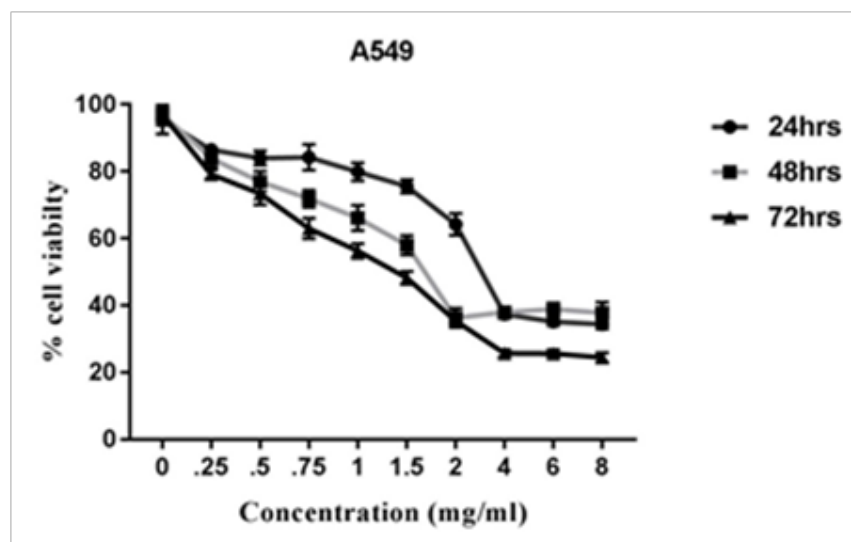
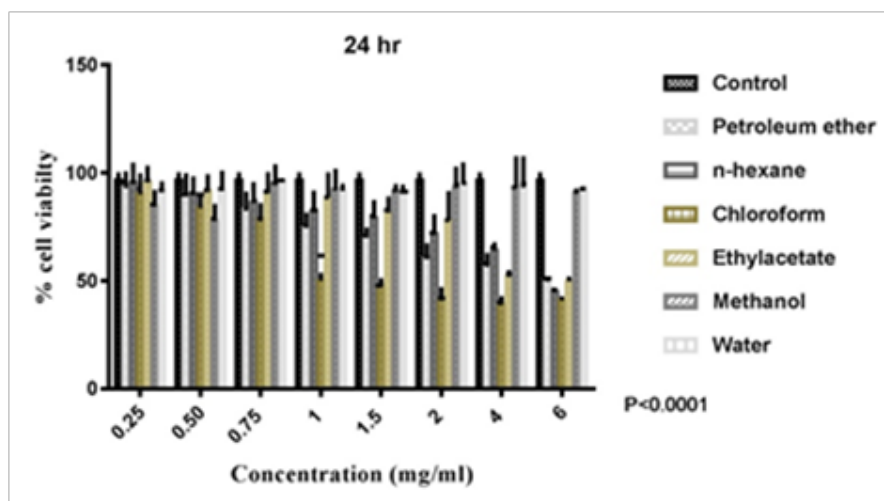
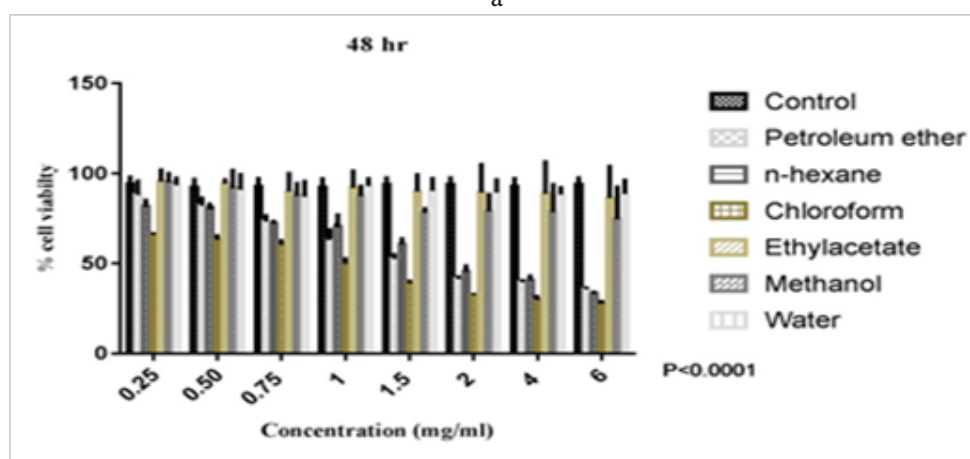


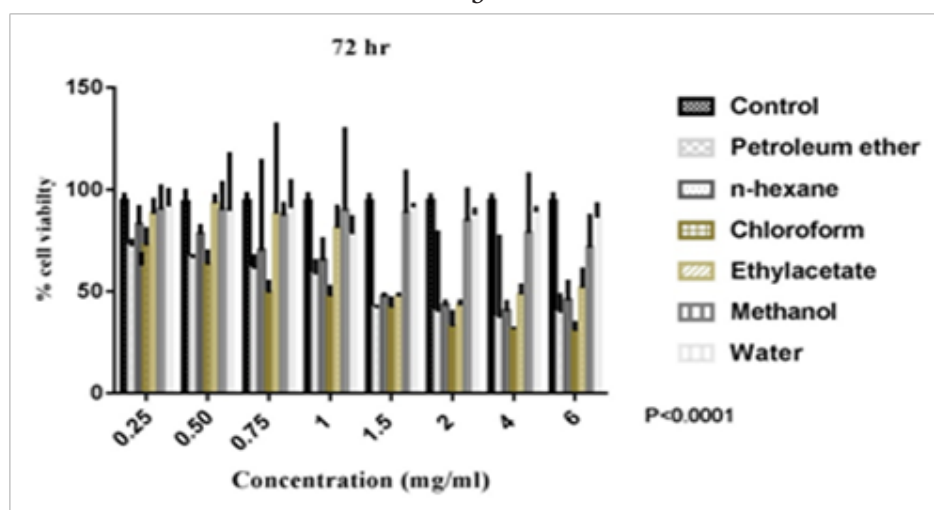
**Figure 4.** IC<sub>50</sub> values of crude petroleum ether bark extract of *Bauhinia variegata* on A549 cells for 24 h, 48 h, and 72 h (n=3).



a



b



c

**Figure 5.** The effect of *Bauhinia variegata* bark extracts against H460 cell line for 24 h, 48 h, and 72 h. Percentage growth proliferation of H460 cells was assayed at 100 mg/ml concentration of extracts using MTT assay as described in the Methods section — **a)** Effect of different concentrations of different bark extracts on H460 cells for 24 h **b)** Effect of different concentrations of different bark extracts on H460 cells for 48 h **c)** Effect of different concentrations of different bark extracts on H460 cells for 72 h respectively. Data represented as the mean  $\pm$  standard deviation of at least three experiments. \*\*\*\*P<0.0001.

cytotoxicity at 24 h treatment. The cytotoxicity of CBE on H460 cells was time dependent demonstrating a potent and definite growth inhibitory effect as shown in Figure 5. The cytotoxicity of CBE on H460 cells increased from 30.9 % to 27.9 % to 26 % after 24, 48 and 72 h respectively. The difference in the behavior of both cell lines may be due to their different molecular characteristics which are targeted by the different phytochemicals present in the two bark extracts (Figure 5 a, b, c).

### 3.3.2 CBE Inhibits Growth and Proliferation of H460 Cells

Examination of H460 cell morphology was done at 24 h treatment of CBE and it was observed that from 0.5, 1, 1.5, 2 mg/ml concentrations, cells had changed morphologically and started to shrink showing the symptoms of the cell death.

The morphological examination of the cells after CBE treatment showed as cell shrinkage and rounding up of the cells which are typical feature of cell death as shown in Figure 6.

### 3.3.3 Determination of IC50 Value of CBE Extract

Effect of different concentrations of CBE of *Bauhinia variegata* on the viability of H460 cells for different time interval (at 24 h, 48 h and 72 h) was assessed. The IC50 values were 1.0 mg/ml for 24 h, 0.78 mg/ml for 48 h and 0.74 mg/ml for 72 h as shown in Figure 7. The extract was more potent after 24 h than after 48 h treatment. The inhibitory concentrations for 24 and 48 h do not show much difference. So, the 24 h treatment was selected for further experiments on H460 cells (Figure 7).

## 3.4. Colony Growth Inhibition Studies - Soft Agar Assay

### 3.4.1 PEBE Inhibits A549 Colony Growth

The ability of PEBE to inhibit the expansion of tumors (cell colonies) and therefore the spread of cancer cells was assayed *in vitro*. PEBE significantly decreased A549 colony growth in a concentration-dependent manner showing significant antitumorigenic activity at 2 mg/ml as shown in Figure 8. The mean tumor diameter in the control (untreated) was 46.2  $\mu\text{m}$ , while at 2 mg/

ml treatment the diameter was reduced to 30.4  $\mu\text{m}$  as shown in Figure 8i. Quantitative analysis of these results is shown in Figure 8ii.

### 3.4.2 CBE Inhibits H460 Colony Growth

CBE significantly decreased colony growth of H460 cells in a concentration-dependent manner with a significant antitumorigenic activity at a concentration of 2 mg/ml Figure 9. The mean tumor diameter for control (untreated) is 63.38  $\mu\text{m}$  which decreased to 27.93  $\mu\text{m}$  in 2 mg/ml concentration treatment and showed a reduction in size of around 33.27  $\mu\text{m}$  in diameter as shown in Figure 9i. Lower concentrations of 1 and 1.5 mg/ml showed no significant difference in mean tumor diameter as compared to control cells. Quantitative analysis of these results is shown in Figure 9ii.

## 3.5 Wound Healing Assay/ Scratch Test

### 3.5.1 PEBE Showed Slower Migration in A549 Treated Cells

Cell migration was investigated by performing the cell scratch assay. In A549 cells, as compared with the control group, gradual reduction was noticed within the number and rate of migrated cells with PEBE treatment. A slower rate of migration was observed with 0.5 and 1 mg/ml PEBE treatment while at 2 mg/ml the cells were unable to survive. Hence, this dose was excluded from the study. The distance was more between the edges of the wound when A549 cells were treated with PEBE for 12 to 36 h, demonstrating the reduced migration of A549 cells as shown in Figure 10i. Quantitative analysis of the scratch diameter is shown in Figure 10ii.

### 3.5.2 CBE Showed Slower Migration in H460 Treated cells

The effect of different concentrations of CBE extract on H460 cells after 24 h treatment indicated a dose-dependent decrease in viability of cells in comparison to control cells. H460 cells also showed slower migration and wound healing with 1 mg/ml and 1.5 mg/ml CBE treatment. CBE impaired cell migration for 12 to 30 h as shown in. The cells lost their viability at 2 mg/ml treatment, and hence this dose was not included for

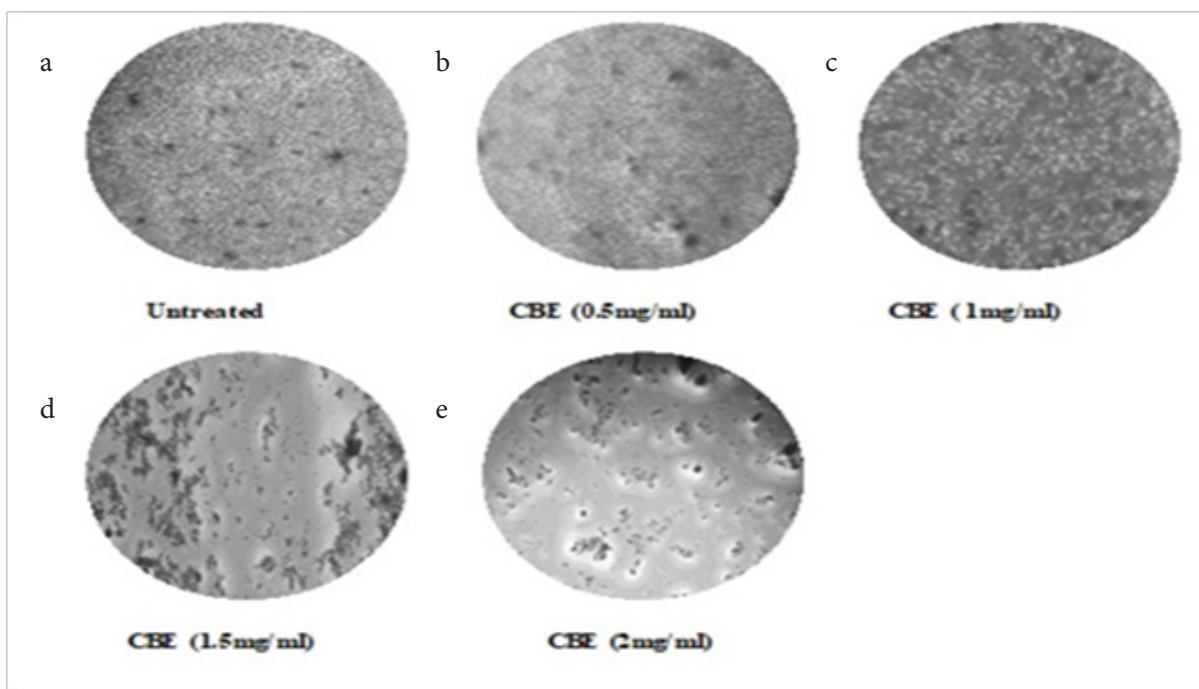


**Figure 6.** Morphological effects of H460 untreated cells **a)** without treatment, and cells exposed to **b)** CBE (0.5 mg/ml), **c)** CBE (1 mg/ml), **d)** CBE (1.5 mg/ml), **e)** CBE (2 mg/ml) of *Bauhinia variegata*.

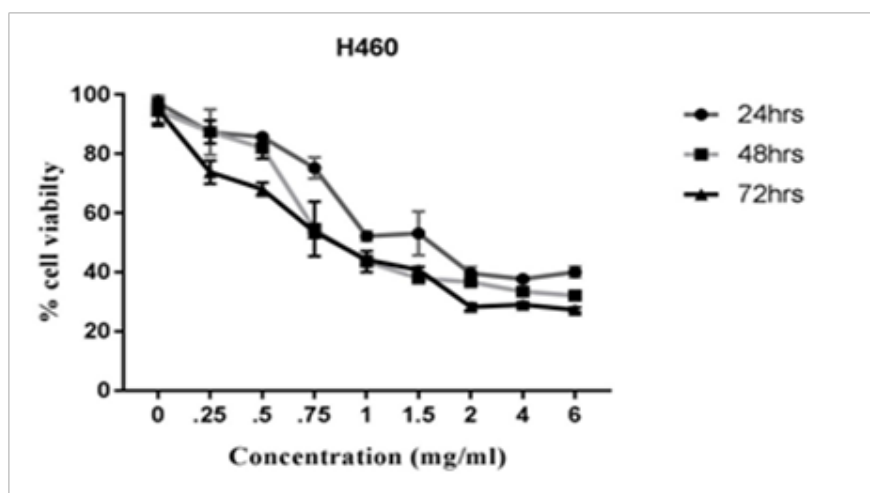


**Figure 7.** IC<sub>50</sub> values of crude chloroform bark extract of *Bauhinia variegata* on H460 cells for 24 h, 48 h, and 72h (n=3).

the comparison as shown in Figure 11i. Quantitative analysis of the scratch diameter is shown in Figure 11 ii.

### 3.6 DNA Fragmentation Studies

#### 3.6.1 PEBE Induces Cellular DNA Fragmentation in A549 Cells

In order to explain the mechanism of cell apoptosis mediated by PEBE, we performed a DNA fragmentation assay, since DNA fragmentation is the characteristic

for apoptosis. Treatment of cells with different concentrations of PEBE for 48 h, led to a decrease in band intensity of DNA with increasing concentration of PEBE in 1 % agarose gel electrophoresis as shown in Figure 12a. A typical DNA ladder pattern of internucleosomal fragmentation was observed with after 48 h of treatment as shown in Figure 12b. The late stages of apoptosis are characterized by damage (fragmentation) of DNA<sup>27</sup>. These data suggest that PEBE extract is an effective inducer of Apoptosis.

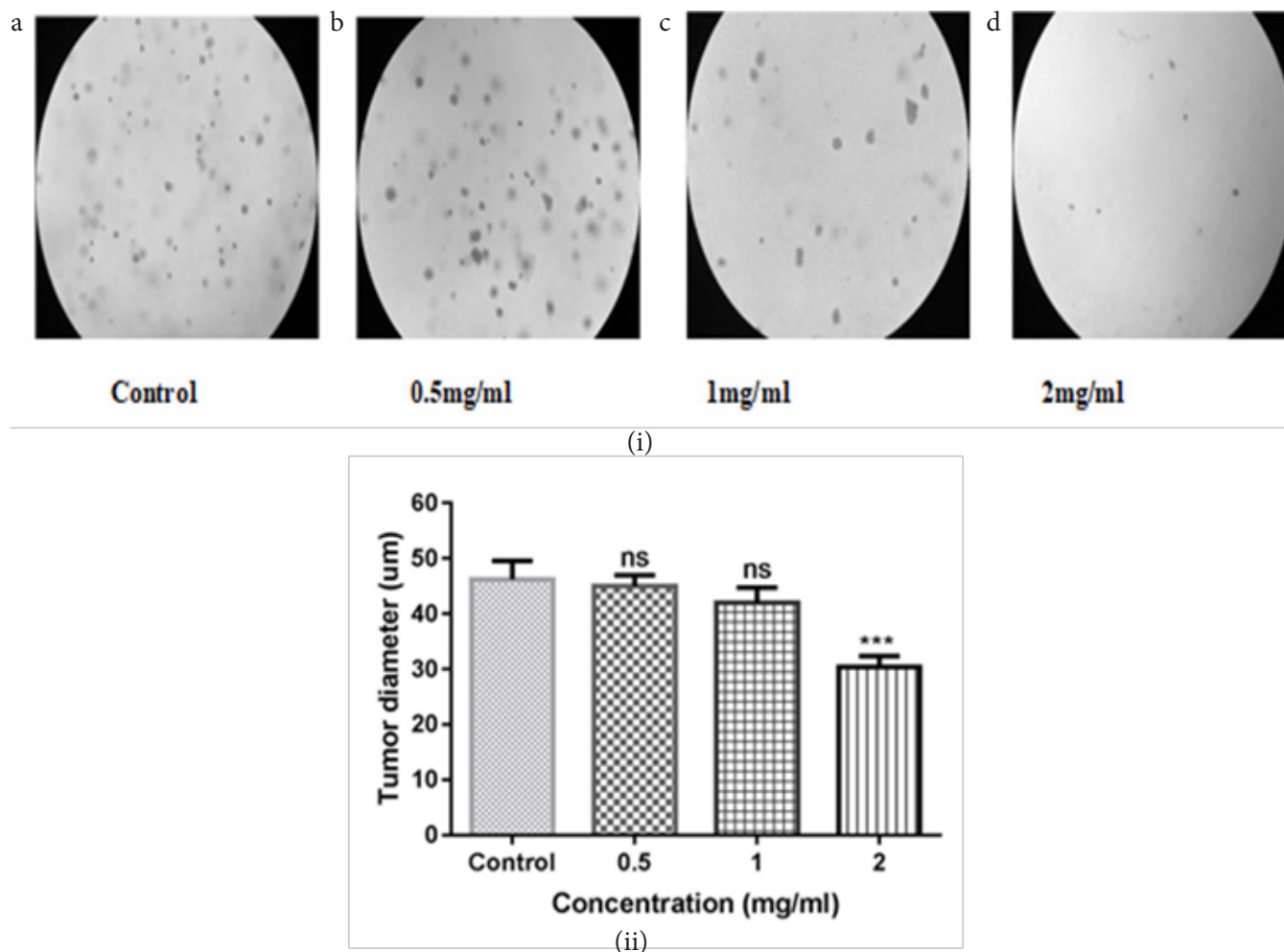


**Figure 8.** Representative images for *in vitro* assay to assess the anti- tumorigenic activity of the PEBE on A549 cells. Cell colonies in soft agar in (i) a) Untreated cells, b) 0.5 mg/ml PEBE treatment, c) 1 mg/ml PEBE treatment, d) 2 mg/ml PEBE treatment; n = 3. Quantitative analysis of mean tumor (colony) diameter of different concentrations of PEBE is shown in (ii) Values are the means  $\pm$  SD of at least three independent experiments; \*\*\*P<0.001, ns = non-significant.

### 3.6.2 CBE Induces Cellular DNA Fragmentation in H460 Cells

Fragmentation of genomic DNA (light fragments) was observed in H460 cell line treated with 2 and 4 mg/ml of CBE for 24 h as shown in Figure 13. A typical ladder pattern of internucleosomal fragmentation was observed in H460 cell line after 24 h at higher concentrations of CBE. Low-molecular-weight DNA from these cells was resolved in 2.0 % agarose gels. These data suggest that CBE is a potent inducer of apoptosis. Further studies are needed to establish the role of the interaction of CBE with DNA in cancer cells.

## 3.7 Quantification of ROS

### 3.7.1 Effects of PEBE on Intracellular ROS Levels of A549 Cells- DCHF-DA Assay

ROS levels were examined at indicated time points (0 to 10 h) after PEBE treatment on A549 cells and it was seen that the ROS levels reached a maximum at about 6 h (29.5 %, as compared to 8 % at 0 h), but subsequently decreased as shown in Figure 14. On treatment with PEBE, intracellular ROS elevates at initial hours and decrease subsequently which suggest they could be activating downstream signaling pathway resulting in apoptosis. These results indicate that ROS production is an early phase event in apoptosis induced by PEBE.

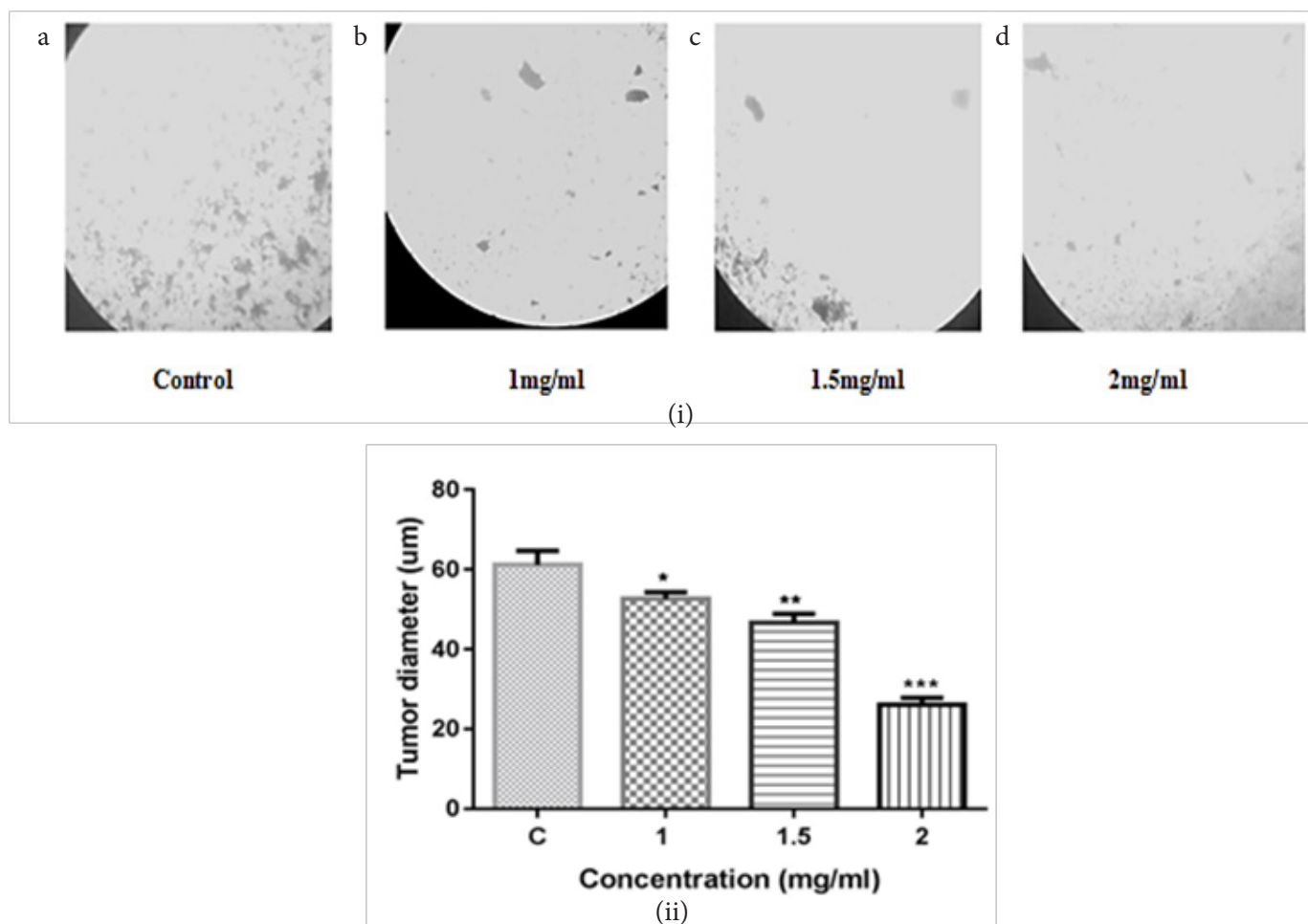


**Figure 9.** Representative images for the *in vitro* assay to assess the anti-tumorigenic activity of the CBE on H460 cells. Cell colonies in soft agar in (i) a) Untreated cells, b) 1mg/ml CBE treatment, c) 1.5 mg/ml CBE treatment, d) 2mg/ml CBE treatment; n = 3. Quantitative analysis of mean tumor (colony) diameter of different concentrations of CBE is shown in (ii) Values are the means  $\pm$  SD of at least three independent experiment: \*\*P<0.01., \*\*\*P<0.001.

### 3.7.2 Effects of CBE on Intracellular ROS Levels of H460 Cells - DCHF-DA Assay

Recent studies have shown that ROS levels in a cell may have a significant role to play in the outcome of therapeutic agents<sup>28</sup>. After exposure of H460 cells to CBE, ROS levels first increase then there is a little decrease at 6h and then stability increase within the cells as shown in Figure 15. Data showed that CBE increased ROS generation from 2 to 10h treatment.

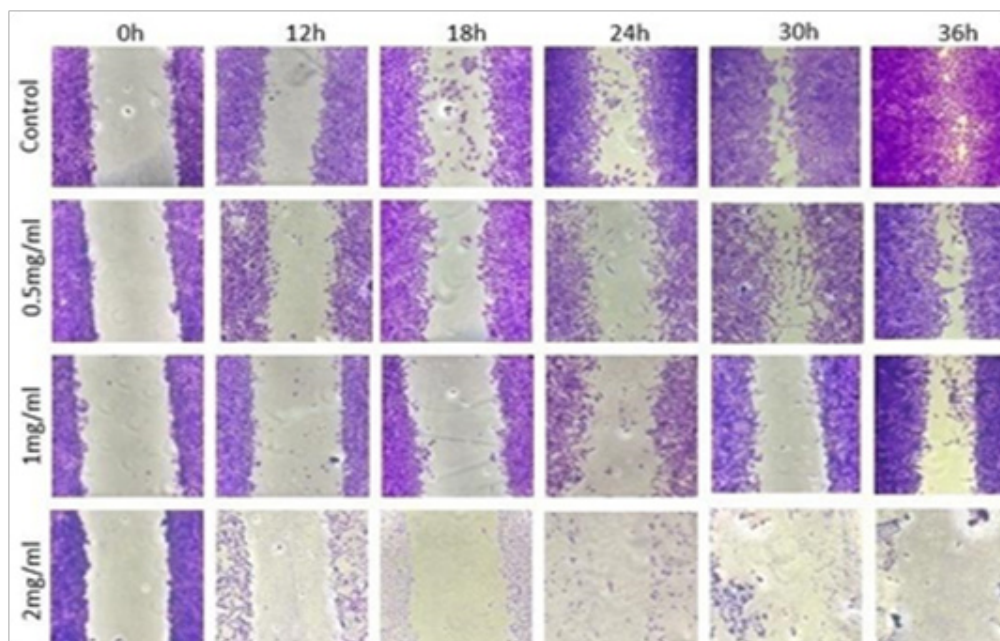
### 3.8 Alterations in Nuclear Morphology - DAPI Staining

DAPI staining was done after treatment of A549 cells with PEBE (1 mg/ml) showed chromatin condensation, nuclear fragmentation (“horse-shoe” like appearance

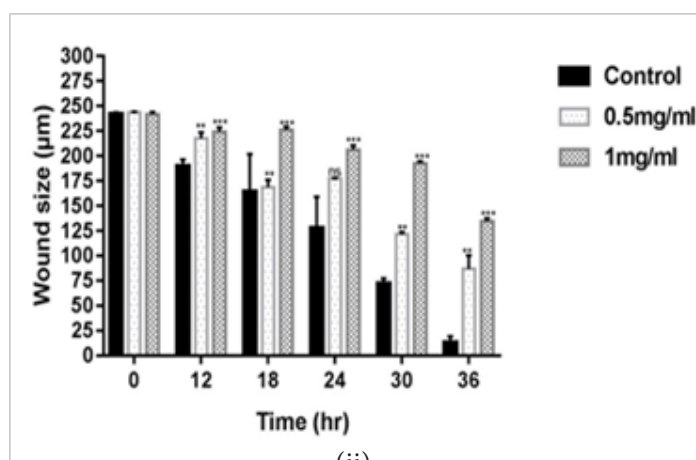
of nucleus) and cell shrinkage with an increase in apoptotic bodies in cells treated with 1.5 mg/ml PEBE for 48 h as shown in Figure 16 a, b, c. The control cells had round homogenous nuclei. The morphological changes associated with apoptosis such as margination of nucleus, chromatin condensation and nuclear fragmentation marked by arrows in Figure 16 d, e, f in H460 cells after 24h treatment with increasing concentrations (IC<sub>50</sub>) of extracts is very distinct.

### 3.9 AO/EtBr Staining

Live cells with normal morphology were abundant in the A549 control group whereas early apoptotic cells were observed on treatment with 1 mg/ml PEBE concentration. Both early and late apoptotic cells were

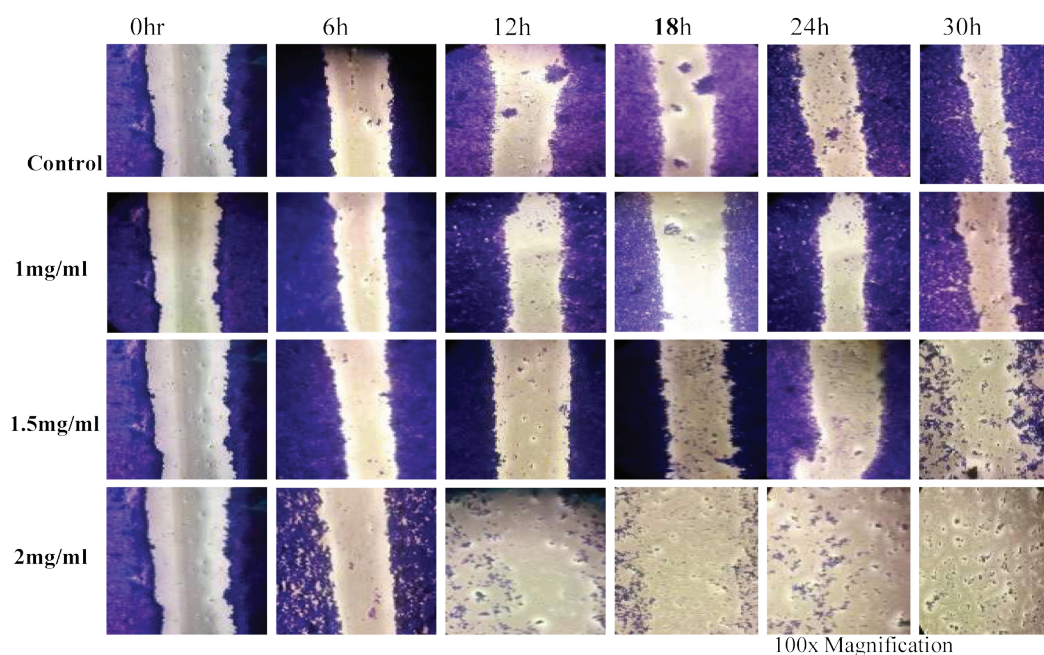


(i)

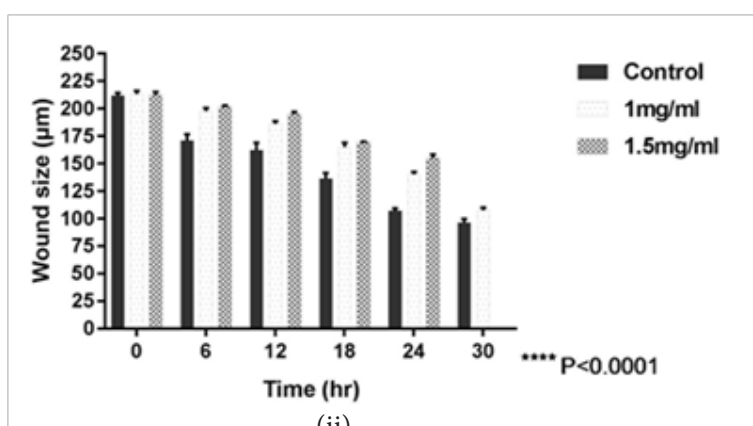


(ii)

**Figure 10.** Representative images are the results of *in vitro* scratch test to assess effect of PEBE on cell migration of A549 cells;  $n = 3$ . PEBE inhibits migration of A549 cells as shown in (i). Wound healing assay to determine the effect of PEBE on A549 cell migration at 0.5, 1, 1.5 and 2mg/ml concentrations for 36h. Quantitative analysis of wound size ( $\mu\text{m}$ ) within 36 h. is represented in (ii). Error bars indicates the standard error of the mean of three independent experiments. \*\* $P < 0.01$ , \*\*\* $P < 0.001$ .

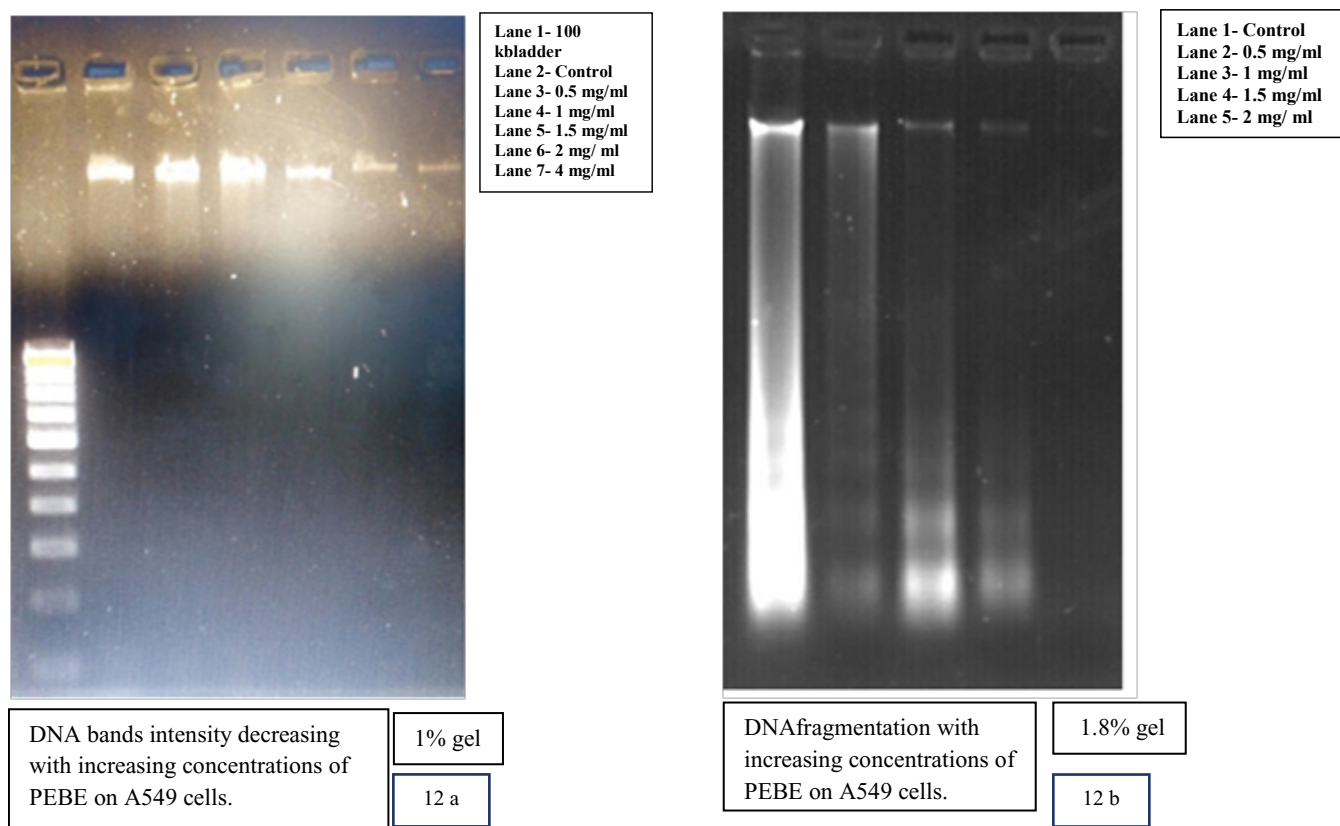


(i)

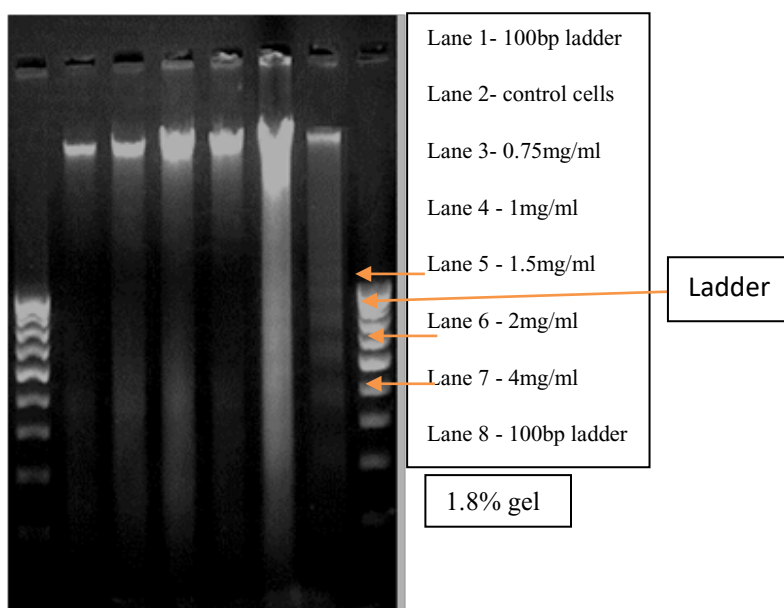


(ii)

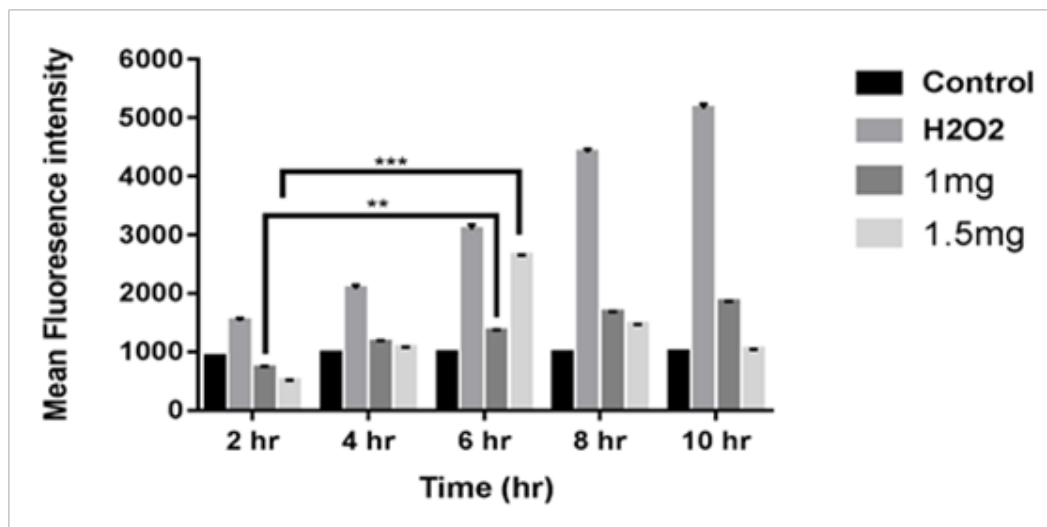
**Figure 11.** Representative images for the results of *in vitro* scratch test to assess effect of CBE on cell migration;  $n = 3$ . CBE inhibits migration of H460 cells (i) Wound healing assay to determine the effect of CBE on H460 cell migration. Quantitative analysis of wound size ( $\mu\text{m}$ ) within 30 h, is measured here in (ii) Error bars indicate the standard error of the mean of three independent experiments:  $***P < 0.001$ .



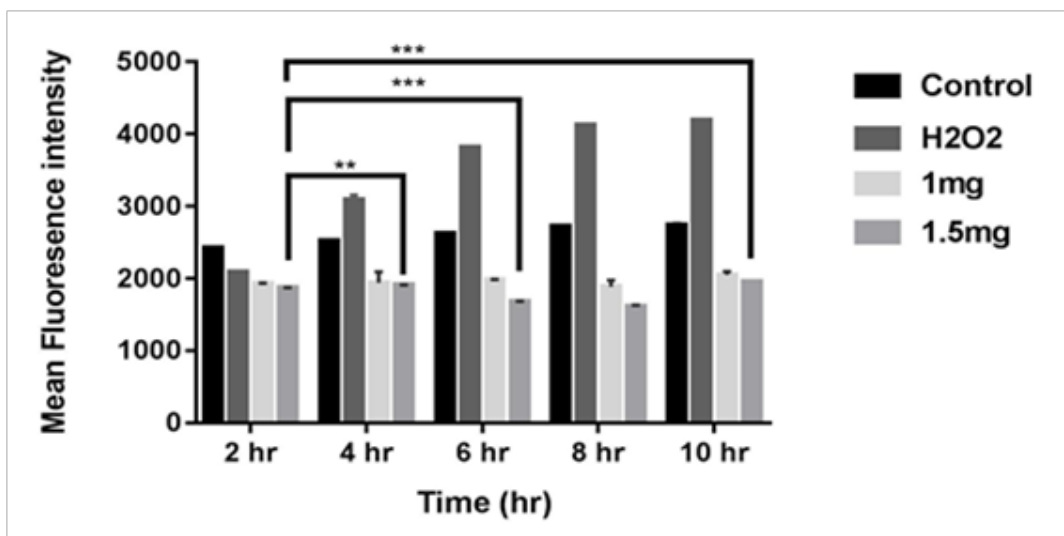
**Figure 12.** Representative images of DNA laddering in A549 cells **(a)** Cells treated with different concentrations of PEBE for 48 h results in decrease in DNA bands with increasing concentration of PEBE in 1% agarose gel electrophoresis, **(b)** Cells treated with increasing concentrations of PEBE for 48 h, and results in typical laddering pattern in 1.8% agarose gel electrophoresis.



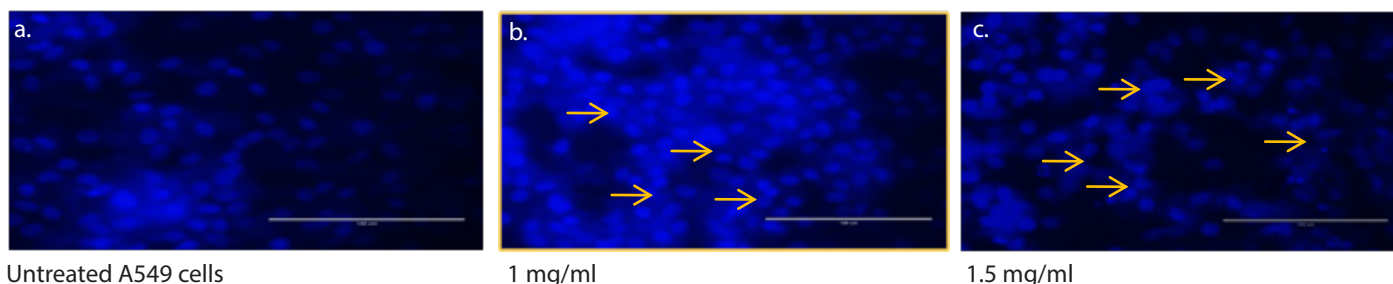
**Figure 13.** Representative images of DNA laddering in H460 cells. Cells treated with increasing concentrations of CBE for 24 h and results in typical laddering pattern in 1.8% agarose gel electrophoresis.

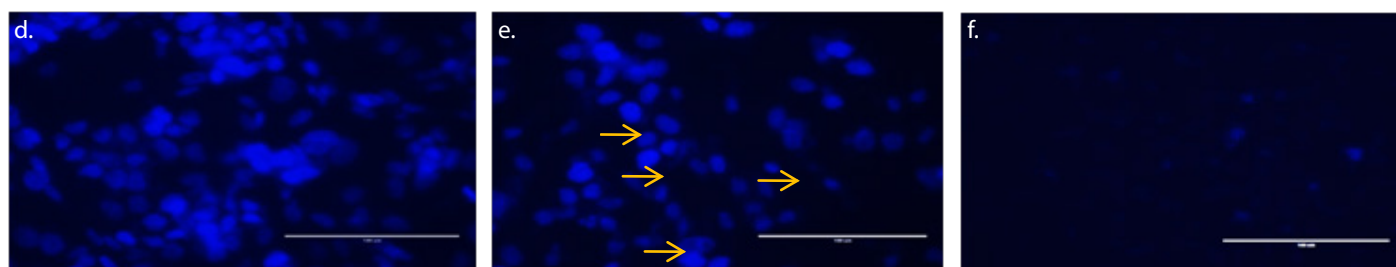


**Figure 14.** Time - dependent changes in ROS levels of A549 cells at different concentrations of PEBE. Data expressed as mean  $\pm$  SEM, \*\* $p < 0.01$ , \*\*\* $p < 0.001$  as compared to control.



**Figure 15.** Time - dependent changes in ROS levels of H460 cells at different concentrations of CBE. Data expressed as mean  $\pm$  SEM, \*\* $p < 0.01$ , \*\*\* $p < 0.001$  as compared to control.



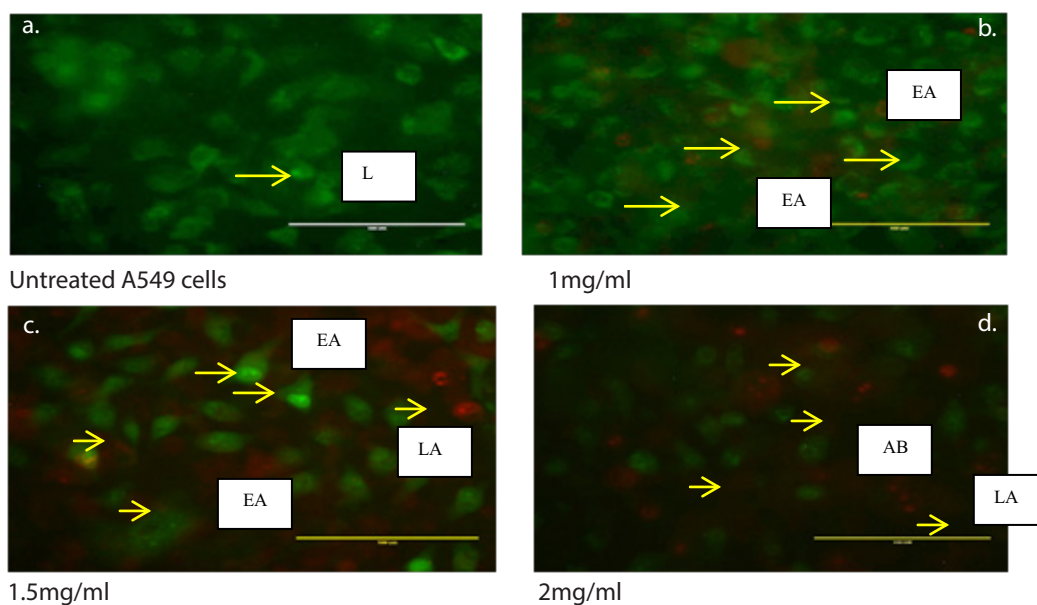


Untreated H460 cells

1 mg/ml

1.5 mg/ml

**Figure 16.** The effect of PEBE on apoptotic potential in A549 cells was evaluated using DAPI staining. **a)** control group; **b)** in the presence of 1 mg/ml; **c)** 1.5mg/ml of PEBE of *Bauhinia variegata* for 48 h under fluorescence microscope, Scale bar-100 um, Mag- 40x. Effect of CBE on apoptotic potential in H460 cells was evaluated using DAPI staining **d)** control H460 cells **e)** 1 mg/ml **f)** 1.5 mg/ml CBE of *Bauhinia variegata* for 24 h under fluorescence microscope, Scale bar-100 um, Mag- 40x. Arrow indicates chromatin condensation, nuclear fragmentation, horse- shoe shape nuclei and cell shrinkage in treated cells as compared to control cells.



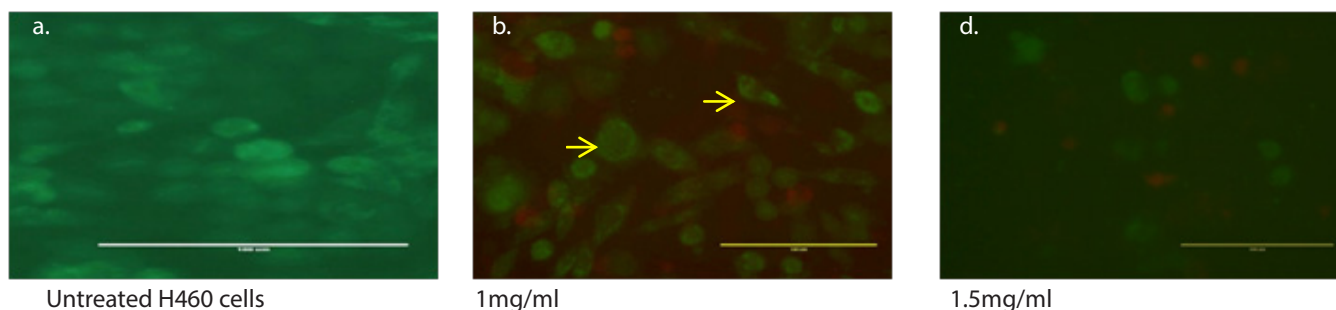
Untreated A549 cells

1mg/ml

1.5mg/ml

2mg/ml

**Figure 17.** A549 cells were stained by AO/EB and observed under fluorescence microscope: **a)** A549 control group; **b)** in the presence of 1 mg/ml; **c)** 1.5mg/ml; **d)** 2mg/ml of PEBE for 48h. Control wells were treated with equivalent amount of medium alone. Green live cells showed normal morphology with uniform nuclei; yellow early apoptotic cells showed nuclear margination and chromatin condensation. Late orange/red apoptotic cells showed fragmented chromatin and apoptotic bodies.



Untreated H460 cells

1mg/ml

1.5mg/ml

**Figure 18.** H460 cells were also stained by AO/EB and observed under fluorescence microscope: **a)** control group; **b)** in the presence of 1 mg/ml; **c)** 1.5mg/ml of CBE for 24h. Green live cells showed normal morphology with uniform nuclei; yellow early apoptotic cells showed nuclear margination and chromatin condensation. Late orange/red apoptotic cells showed fragmented chromatin and apoptotic bodies.

observed in A549 cell line treated with 1, 1.5 and 2 mg/ml concentrations. The 2 mg/ml treatment showed the greatest number of apoptotic bodies, and the cells were mostly in the late apoptotic stage as shown by arrows in Figure 17 a, b, c, d. Live cells appeared green, while early apoptotic appeared bright green or yellow and late apoptotic appeared red with condensed and fragmented nuclei.

For H460 cell line, live cells with normal morphology were abundant in H460 control group. H460 cell line treated with 1 mg/ml CBE showed early apoptotic cells while H460 cell line treated with 1.5 mg/ml CBE

showed late apoptotic bodies as shown in Figure 18 a, b, c.

### 3.10 Caspase-3 Activity in Cell Lines after PEBE and CBE Treatment

Caspase-3, a marker of apoptosis and has shown to be adequate for potent activation of apoptosis<sup>29,30</sup>. Caspase 3 activity significantly increased in PEBE treated A549 cells and CBE treated H460 cells at the IC<sub>50</sub> value after 24 h to 48 h treatment. After 48 h of incubation of A549 cell line with PEBE there was a 3-fold increase in

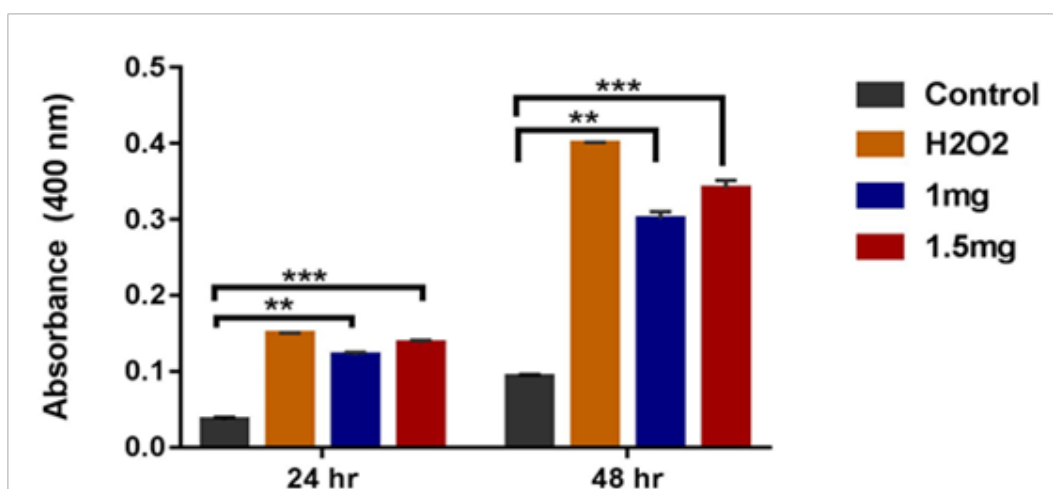


**Figure 19.** A549 cells were seeded in 24 well plates, then treated with PEBE in concentration and time - dependent manner. Caspase-3 activity were measured spectrophotometrically by detection of chromophore pNA at 405nm. Data expressed as mean  $\pm$  SEM, n=3 \*\*p < 0.01, \*\*\*p < 0.001 as compared to control.

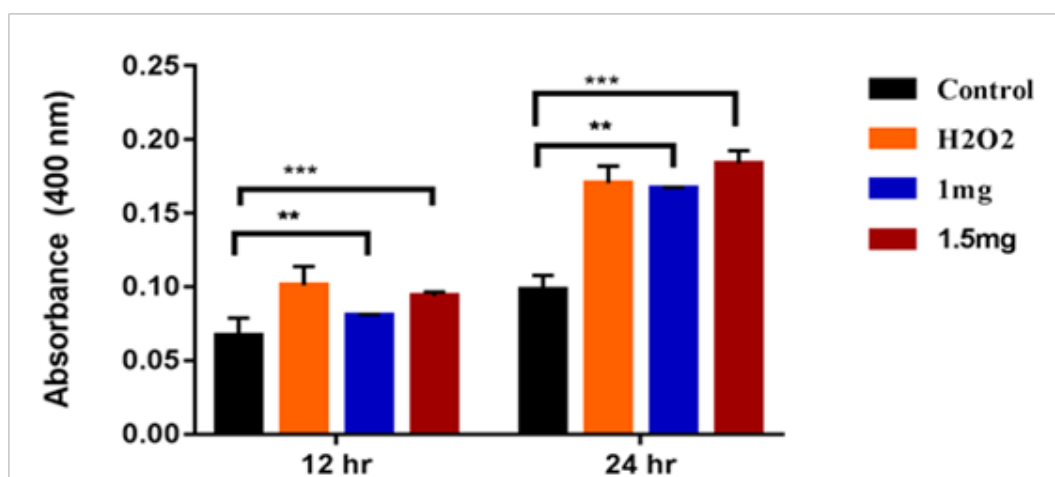


**Figure 20.** H460 cells were seeded in 24 well plates, then treated with CBE in concentration and time - dependent manner. Caspase-3 activity were measured spectrophotometrically by detection of chromophore pNA at 405nm. Data expressed as mean  $\pm$  SEM, n=3 \*\*p < 0.01, \*\*\*p < 0.001 as compared to control.

caspase-3 levels as compared to A549 control cells as shown in Figure 19.

Caspase-3 activity significantly increased at IC<sub>50</sub> value of CBE from 12 h to 24 h treatment in H460 cell line as shown in Figure 20. From these data, we can say that Caspase-3 may also function before or at the stage when commitment to loss of cell viability is made.

### 3.11 Alteration in Mitochondrial Membrane Potential by TMRM Staining

Cell health can be assessed by proper functioning of mitochondria which can be monitored by observing changes in mitochondrial membrane potential (MMP). The role of intrinsic apoptosis pathway was further

validated by the changes in mitochondrial membrane potential in A549 cells treated with PEBE (1 mg, 1.5 mg) for 48 h and H460 cells treated with CBE at (1 mg, 1.5 mg) for 24 h. PEBE and CBE significantly decreased the mitochondrial membrane potential ( $\Delta\Psi_m$ ) in A549 as shown in Figure 21 a, b, c and H460 cells as shown in Figure 21 d, e, f with increasing concentrations.

## 4. Discussion

Our data validates with proof of mechanism demonstrating the efficacy of *Bauhinia variegata* PEBE against A549 cells proliferation and CBE against H460 cells thus targeting two types of lung cancer cell lines widely used for such studies<sup>31,32</sup>. We demonstrate potent antiproliferative activity with very low antioxidant

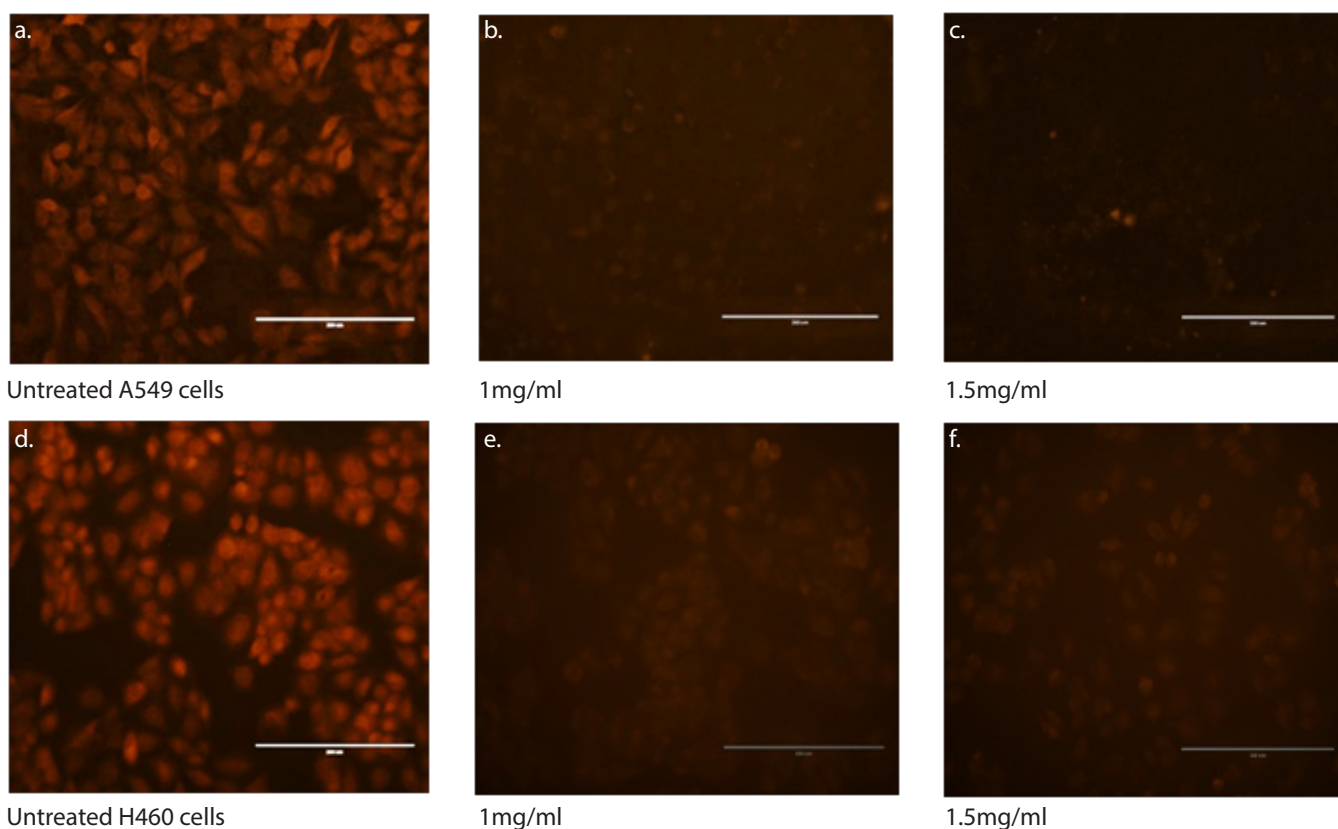


**Figure 21.** Cells were stained with TMRM and imaged by standard fluorescence techniques. PEBE (1 mg/ml, 1.5 mg/ml) for 48 h did not show significant change in TMRM fluorescence intensity in A549 cells (a - c), while CBE (1 mg/ml, 1.5 mg/ml) for 24 h significantly decreased TMRM fluorescence intensity in H460 cells (d - f).

capacity indicating its function via modulation of cellular redox status.

All of the *Bauhinia variegata* bark extracts were differently inhibiting A549 cells proliferation but petroleum ether extract was found to be the foremost potent inhibitor of A549 cells proliferation at 48 h treatment which was estimated by MTT assay (Figure 2) with IC<sub>50</sub> of 1.5 mg/ml at 48 h treatment (Figure 4). The IC<sub>50</sub> value of PEBE was determined and guided the treatment design. The ability of PEBE to inhibit the expansion of tumors (cell colonies) and therefore the spread of cancer cells was assayed *in vitro*. We next assessed the effect of PEBE treatment on Clonogenic survival of the A549 cells. Clonogenic study revealed that PEBE showed significant anti-tumorigenic activity as shown in (Figure 8) and (Figure 10) showed a depreciation in the wound closure ability of A549 cells after treatment in time and dose dependent manner as compared to the control cells. The study also tried to probe into the molecular mechanism behind the cytotoxic effect of PEBE. Cytoarchitectural changes due to DNA fragmentation is one of the hallmarks of apoptotic pathway. Treatment with PEBE showed a decrease in DNA bands (Figure 12a) and fragmentation of genomic DNA was observed at 48 h treatment (Figure 12b). Increase in ROS levels in cancer cells may contribute to the biochemical and molecular changes necessary for tumor initiation, promotion, progression,

and chemoresistance. The pattern of changes in ROS level was monitored (Figure 14) as it has a bearing on the drug sensitivity of the cell towards anticancer compounds. This result indicates that ROS production is an early phase in apoptosis induced by PEBE treatment. The morphological changes were detected by DAPI staining (Figure 16 a, b, c) and AO/EtBr staining as shown in (Figure 17 a, b, c, d). Caspase-3, an important effector of apoptosis got activated by PEBE treatment on A549 cells after 48 h (Figure 19). The decrease in MMP of A549 cells treated with various concentrations of PEBE was observed using TMRM dye (Figure 21a, b, c as compared to control cells showing the occurrence of apoptosis.

Comparative studies were also carried out in H460 cells (large cell carcinoma). All of the *Bauhinia variegata* bark extracts were differently inhibiting H460 cells proliferation but chloroform bark extract was found to be the foremost potent inhibitor of H460 cells proliferation followed by petroleum ether bark extract as shown in (Figure 5) with IC<sub>50</sub> of 1 mg/ml at 24 h (Figure 7). Clonogenic ability of CBE shows significant difference in mean tumor diameter as shown in (Figure 9) and slower migration and wound healing was observed in (Figure 11) as compared to H460 control cells. CBE acted *via* the apoptotic pathway & showed fragmentation of genomic DNA in dose and time dependent manner (Figure 13). Increase in ROS was

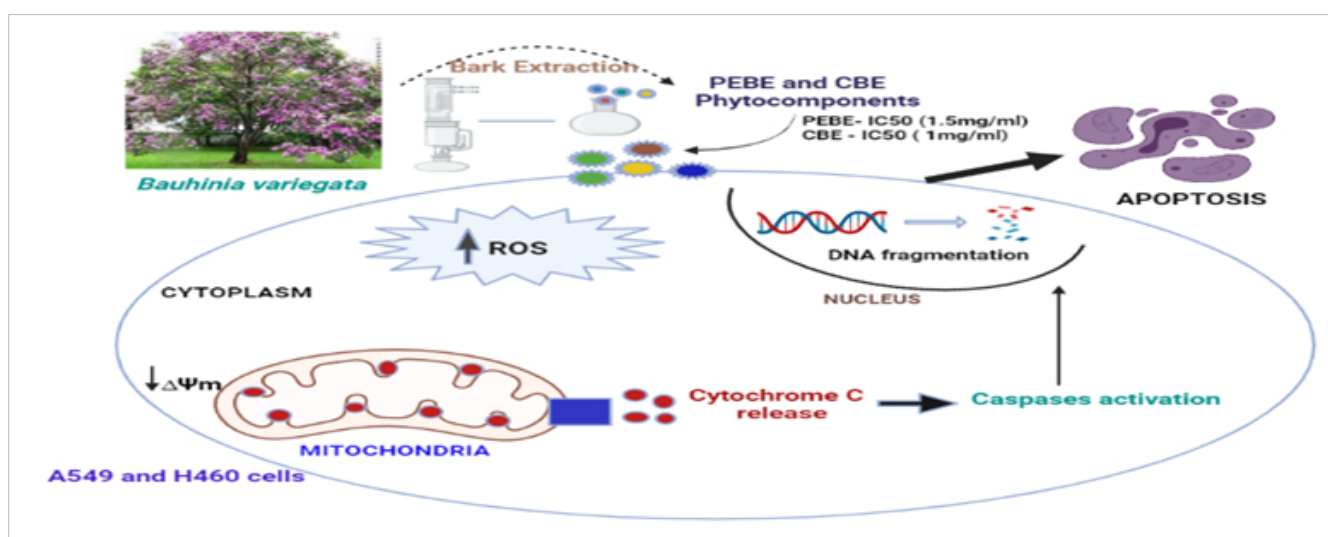


**Figure 22.** Proposed signaling pathways activated by Petroleum ether and Chloroform bark extracts of *Bauhinia variegata* leading to the observed anticancer effect.

responsible for CBE-induced apoptosis in H460 cell line (Figure 15). Morphological changes in apoptotic cells were detected by DAPI staining (Figure 16 d, e, f) and AO/EtBr staining as shown in (Figure 18 a, b, c). Unraveling the molecular mechanism showed that CBE causes the activation of caspase-3 in H460 cells at 24 h treatment. Further, there is a decrease in MMP of H460 cells treated with various concentrations of CBE as compared to untreated cells, which was observed using TMRM dye.

PEBE and CBE induced apoptosis of A549 and H460 cell lines may be through the activation of caspase-3 signaling and mitochondrial cell death mediated pathway, leading to the observed anti cancerous effect as shown in Figure 22. Our data suggest that PEBE and CBE possess strong antiproliferative effects against lung cancer cells with low toxicity. Plants are such a repertoire of molecules with phenomenal properties waiting to be unraveled. Study like this may seem like a drop in the ocean but they are necessary in retaining a hope for an alternative drug for the cancer treatment.

## 5. Conclusion

Thus, it can be concluded that phytocomponents from *Bauhinia variegata* hindered a normal growth of A549 and H460 cancer cell lines by inducing apoptosis, inhibiting colony formation, decreasing cell migration, increasing intracellular ROS levels, activating Caspases and decreasing Mitochondrial matrix potential. We have narrowed down on few phytocomponents by GC-MS analysis and one of this could be a strong contender for treatment of this disease.

## 6. Acknowledgement

TK did most of the experiments, AD helped in data analysis, JV and DJ helped with some experiments, SP helped in establishing the cell culture facility, PR conceptualized the project. We thank the Forest Officer, Waghai Botanical Garden, for permission to collect samples. The project was supported by research grant to PR and fellowship to TK by Gujarat State Biotechnology Mission, Gandhinagar, India.

## 7. References

1. Parikh PM, Ranade AA, Govind B, Ghadyalpatil N, Singh R, Bharath R, *et al.* Lung cancer in India: Current status and promising strategies. *South Asian J Cancer.* 2016; 5(03):093-5. <https://doi.org/10.4103/2278-330X.187563>. PMID:27606289. PMCID:PMC4991145
2. Zappa C, Mousa SA. Non-small cell lung cancer: Current treatment and future advances. *Transl Lung Cancer Res.* 2016; 5(3):288. <https://doi.org/10.21037/tlcr.2016.06.07>. PMID:27413711. PMCID:PMC4931124
3. Lu T, Yang X, Huang Y, Zhao M, Li M, Ma K, *et al.* Trends in the incidence, treatment, and survival of patients with lung cancer in the last four decades. *Cancer Manag Res.* 2019; 11:943. <https://doi.org/10.2147/CMAR.S187317>. PMID:30718965. PMCID:PMC6345192
4. Debevec L, Debeljak A. Multidisciplinary management of lung cancer. *J Thorac Oncol.* 2007; 2(6):577. <https://doi.org/10.1097/JTO.0b013e318060f16d>. PMID:17545858
5. Huang CY, Ju DT, Chang CF, Reddy PM, Velmurugan BK. A review on the effects of current chemotherapy drugs and natural agents in treating non-small cell lung cancer. *Biomedicine.* 2017; 7(4). <https://doi.org/10.1051/bmdcn/2017070423>. PMID:29130448. PMCID:PMC5682982
6. Jin S, Park HJ, Oh YN, Kwon HJ, Kim JH, Choi YH, *et al.* Anti-cancer activity of *Osmanthus matsumuranus* extract by inducing G2/M arrest and apoptosis in human hepatocellular carcinoma Hep G2 cells. *J Cancer Prev.* 2015; 20(4):241. <https://doi.org/10.15430/JCP.2015.20.4.241>. PMID:26734586. PMCID:PMC4699751
7. Richardson JS, Sethi G, Lee GS, Malek SN. Chalepin: isolated from *Ruta angustifolia* L. Pers induces mitochondrial mediated apoptosis in lung carcinoma cells. *BMC Complement Altern Med.* 2016; 16(1):1-27. <https://doi.org/10.1186/s12906-016-1368-6>. PMID:27729078. PMCID:PMC5059921
8. Mali RG, Dhake AS. Evaluation of effects of *Bauhinia variegata* stem bark extracts against milk-induced eosinophilia in mice. *J. Adv. Pharm. Technol. Res.* 2011; 2(2):132. <https://doi.org/10.4103/2231-4040.82949>. PMID:22171306. PMCID:PMC3217693
9. Katoch D, Sharma JS, Banerjee S, Biswas R, Das B, Goswami D, *et al.* Government policies and initiatives for development of Ayurveda. *J Ethnopharmacol.* 2017; 197:25-31. <https://doi.org/10.1016/j.jep.2016.08.018>. PMID:27543425
10. Aggarwal V, Tuli HS, Varol A, Thakral F, Yerer MB, Sak K, *et al.* Role of reactive oxygen species in cancer progression: Molecular mechanisms and recent advancements. *Biomolecules.* 2019; 9(11):735. <https://doi.org/10.3390/biom9110735>. PMID:31766246. PMCID:PMC6920770

11. Galadari S, Rahman A, Pallichankandy S, Thayyullathil F. Reactive oxygen species and cancer paradox: To promote or to suppress? *Free Radic Biol Med.* 2017; 104:144-64. <https://doi.org/10.1016/j.freeradbiomed.2017.01.004>. PMID:28088622
12. Kirtonia A, Sethi G, Garg M. The multifaceted role of reactive oxygen species in tumorigenesis. *Cell Mol Life Sci.* 2020;1-25.
13. Hensley P, Mishra M, Kyprianou N. Targeting caspases in cancer therapeutics. *Biol. Chem.* 2013; 394(7):831-43. <https://doi.org/10.1515/hsz-2013-0128>. PMID:23509217. PMCid:PMC3721733
14. Jelínek M, Balušíková K, Schmiedlová M, Němcová-Fürstová V, Šrámek J, Stančíková J, et al. The role of individual caspases in cell death induction by taxanes in breast cancer cells. *Cancer Cell Int.* 2015; 15(1):1-6. <https://doi.org/10.1186/s12935-015-0155-7>. PMID:25685064. PMCid:PMC4329194
15. Olsson M, Zhivotovsky B. Caspases and cancer. *Cell Death Differ.* 2011; 18(9):1441-9. <https://doi.org/10.1038/cdd.2011.30>. PMID:21455218. PMCid:PMC3178435
16. Khazaei M, Pazhouhi M. Antiproliferative effect of *Trifolium pratense* L. extract in human breast cancer cells. *Nutr Cancer.* 2019; 71(1):128-40. <https://doi.org/10.1080/01635581.2018.1521443>. PMID:30596276
17. Bhandari J, Muhammad B, Thapa P, Shrestha BG. Study of phytochemical, anti-microbial, anti-oxidant, and anti-cancer properties of *Allium wallichii*. *BMC Complement Altern Med.* 2017; 17(1):1-9. <https://doi.org/10.1186/s12906-017-1622-6>. PMID:28178952. PMCid:PMC5299666
18. Kothari S, Mishra V, Bharat S, Tonpay SD. Antimicrobial activity and phytochemical screening of serial extracts from leaves of *Aegle marmelos* (Linn.). *Acta Pol. Pharm.* 2011; 68(5):687-92.
19. Zhao T, Pan H, Feng Y, Li H, Zhao Y. Petroleum ether extract of *Chenopodium album* L. prevents cell growth and induces apoptosis of human lung cancer cells. *Exp Ther Med.* 2016; 12(5):3301-7. <https://doi.org/10.3892/etm.2016.3765>. PMID:27882153. PMCid:PMC5103781
20. Franken NA, Rodermond HM, Stap J, Haveman J, Van Bree C. Clonogenic assay of cells in vitro. *Nat Protoc.* 2006; 1(5):2315-9. <https://doi.org/10.1038/nprot.2006.339>. PMID:17406473
21. Liang CC, Park AY, Guan JL. In vitro scratch assay: A convenient and inexpensive method for analysis of cell migration in vitro. *Nat Protoc.* 2007; 2(2):329-33. <https://doi.org/10.1038/nprot.2007.30>. PMID:17406593
22. Liu N, Li Y, Su S, Wang N, Wang H, Li J. Inhibition of cell migration by ouabain in the A549 human lung cancer cell line. *Oncol Lett.* 2013; 6(2):475-9. <https://doi.org/10.3892/ol.2013.1406>. PMID:24137350. PMCid:PMC3789103
23. Hsia TC, Yu CC, Hsu SC, Tang NY, Lu HF, Huang YP, et al. Cantharidin induces apoptosis of H460 human lung cancer cells through mitochondria-dependent pathways. *Int J Oncol.* 2014; 45(1):245-54. <https://doi.org/10.3892/ijo.2014.2428>. PMID:24818581
24. Lin W, Ye H. Anticancer activity of ursolic acid on human ovarian cancer cells via ROS and MMP mediated apoptosis, cell cycle arrest and downregulation of PI3K/AKT pathway. *J Buon.* 2020; 25(2):750-56.
25. Alizadeh J, Zeki AA, Mirzaei N, Tewary S, Moghadam AR, et al. Mevalonate cascade inhibition by simvastatin induces the intrinsic apoptosis pathway via depletion of isoprenoids in tumor cells. *Sci Rep.* 2017; 7(1):1-4. <https://doi.org/10.1038/srep44841>. PMID:28344327. PMCid:PMC5366866
26. Bang M, Do Gyeong Kim EL, Kwon KJ, Shin CY. Etoposide induces mitochondrial dysfunction and cellular senescence in primary cultured rat astrocytes. *Biomol Ther.* 2019; 27(6):530. <https://doi.org/10.4062/biomolther.2019.151>. PMID:31646843. PMCid:PMC6824621
27. Elmore S. Apoptosis: A review of programmed cell death. *Toxicol Pathol.* 2007; 35(4):495-516. <https://doi.org/10.1080/01926230701320337>. PMID:17562483. PMCid:PMC2117903
28. Perillo B, Di Donato M, Pezone A, Di Zazzo E, Giovannelli P, Galasso G, et al. ROS in cancer therapy: The bright side of the moon. *Exp Mol Med.* 2020; 52(2):192-203. <https://doi.org/10.1038/s12276-020-0384-2>. PMID:32060354. PMCid:PMC7062874
29. Clark AC, MacKenzie SH. Targeting cell death in tumors by activating caspases. *Curr Cancer Drug Targets.* 2008; 8(2):98-109. <https://doi.org/10.2174/156800908783769391>. PMID:18336192. PMCid:PMC3119715
30. Kumar S. Caspase function in programmed cell death. *Cell Death Differ.* 2007; 14(1):32-43. <https://doi.org/10.1038/sj.cdd.4402060>. PMID:17082813
31. Ji BC, Yu CC, Yang ST, Hsia TC, Yang JS, Lai KC, et al. Induction of DNA damage by deguelin is mediated through reducing DNA repair genes in human non-small cell lung cancer NCI-H460 cells. *Oncol. Rep.* 2012; 27(4):959-64. <https://doi.org/10.3892/or.2012.1622>. PMID:22227970. PMCid:PMC3583480
32. Tiloke C, Phulukdaree A, Chuturgoon AA. The antiproliferative effect of *Moringa oleifera* crude aqueous leaf extract on cancerous human alveolar epithelial cells. *BMC Complement Altern Med.* 2013; 13(1):1-8. <https://doi.org/10.1186/1472-6882-13-226>. PMID:24041017. PMCid:PMC3852616

# Phytochemical evaluation and Chemical characterization of *Bauhinia variegata* L. bark extract by TGA/DSC, FT-IR and GC-MS analytical techniques: Pharmaceutical Aspects

Khanna Tanvi, Dave Akash and Robin Pushpa\*

Department of Biochemistry, The Maharaja Sayajirao University of Baroda, Vadodara, Gujarat, 390002, INDIA

\*pushparobin@gmail.com

## Abstract

*Bauhinia variegata* (Linn.), *Caesalpiniaceae*, known as *Kachnar* in Ayurvedic texts has been shown to have promising anticancer potential. The presence of bioactive molecules in plants which can be commercialized has led to research in knowing their chemical properties. Previous studies from our laboratory have validated the claim of anticancer property of *Bauhinia variegata* by providing biochemical evidence for the effect of petroleum ether bark extract (PEBE) and chloroform bark extract (CBE) on A549 and H460 lung cancer cell lines respectively. This work aimed at the application of various analytical techniques (thermal analysis, Fourier infrared transform spectroscopy and GC-MS) in the characterization of dried extracts of *Bauhinia variegata* with medicinal properties. TG-DSC-FTIR-GC-MS was applied to monitor the thermal stability and chemical properties of *Bauhinia variegata* bark extracts.

The TG analysis of PEBE and CBE showed mass loss within three steps in different temperature ranges. The DSC curves for the dried extracts of *Bauhinia variegata* showed that thermal processes occur between 50 – 100°C for PEBE and 50-70°C for CBE. The FTIR spectroscopic studies of petroleum ether and chloroform bark extracts of *Bauhinia variegata* revealed different characteristic peak values with various functional groups in the extracts. The GC-MS study of PEBE revealed 18 compounds and CBE revealed 8 compounds. Thus, we have been successful in narrowing down to very few probable anticancer compounds from *Bauhinia variegata* bark extracts and also through this study, it was possible to substantiate the possibility of applying these techniques for use in the herbal medicines production from medicinal plants.

**Keywords:** Dried *Bauhinia variegata* bark extract, Thermal analysis, FTIR, GC-MS.

## Introduction

Despite advancements in medicine, a treatment for cancer eludes mankind. Though a plethora of drugs that will help

fight against cancer exist, problems of side effects and multi-drug resistance limit their use. Natural products from plants can help overcome this limitation. *Bauhinia variegata*, known as *Kachnar* in Indian Ayurvedic texts, is a tree found in northern parts of India. In traditional system of medicines like Ayurveda, Unnani, it is used as medicine for basic health care<sup>8</sup>. *Bauhinia variegata* is used as traditional medicine in the treatment of liver disorders, cancer, diabetes<sup>3,4,10,11</sup>.

Previous reports have shown various pharmacological activities like antidiabetic, antitumor, antimicrobial, anti-inflammatory etc<sup>5,9,11</sup>. Literature also showed that *Bauhinia variegata* leaf extracts exhibit antibacterial activity and possessed better antioxidant potential<sup>2</sup>.

The presence of varied compounds in *Bauhinia variegata* flower as well as bark extracts showing different pharmacological activities has been reported<sup>3,11</sup>. There are only a couple of preliminary studies reporting anticancer potential for this plant but ayurvedic texts have mentioned of it. Our laboratory has tried to validate the claim of anticancer property of *Bauhinia variegata* by providing biochemical evidence for the effect of petroleum ether bark extract (PEBE) and chloroform bark extract (CBE) on A549 and H460 lung cancer cell lines respectively. So, it interested us to look at these extracts in modern science perspective.

Thermal analysis has become a significant tool for characterization of dry extracts and plant products. TG alongside other techniques helps in better understanding of the organic molecules especially if the compounds are intended for pharmaceutical use<sup>2</sup>. FTIR analysis will help reveal the chemical composition. Many authors have shown applications of different thermal analysis techniques in pharmaceutical technology and the standardization and characterization of dried extracts of medicinal plants<sup>5,12</sup>.

The method of drug treatment aims at finding a product which attends market necessities as well as provides efficacy, safety and quality. This thermal analysis is going to be useful in studying the behavior of drugs degradation during its dumping process after its expiration since it may also release some toxic by products which may be harmful for the society. The objective of this study was to characterize the dried extracts of *Bauhinia variegata* by TG/DSC analysis and FTIR coupled with GC-MS (TG-DSC-FTIR-GC-MS).

## Material and Methods

**Herbal Material:** Fresh *Bauhinia variegata* bark was collected from Waghai Botanical Garden, Dang, Gujarat in the month of Dec – Jan per annum. The identification was validated by experts of Botany Department at The Maharaja Sayajirao University of Baroda. The bark was washed and surface sterilized with 0.1% mercury chloride, rinsed and kept for shade drying. The bark was then powdered employing a grinder and packed into a thimble for extraction by Soxhlet extraction method with different solvents of accelerating polarity for 8-12 hours<sup>7</sup>.

**Qualitative Phytochemical Screening:** Phytochemical screening of *B. variegata* bark extracts was performed for the qualitative detection of phytochemicals using standard procedures<sup>1</sup>.

**Thermal analysis parameters (TGA/ DSC):** The analysis of the change within the mass of a sample on heating is understood as thermogravimetric analysis (TG). For TGA procedure, about 4 mg of PEBE and CBE samples were analyzed within the temperature interval 30–600 °C with a continuing heating rate of 10 °C /min using Al<sub>2</sub>O<sub>3</sub> crucible under a nitrogen flow of 50 ml/min<sup>9</sup> during a NETZSCH STA 449F3Jupiter. 2005). All mass loss percentages were determined using Proteus analysis software. The DSC curves of PEBE and CBE were obtained during a NETZSCH DSC 200F3 Maia, using PAN aluminum crucibles with about 3-4 mg of samples under nitrogen atmosphere at the flow of 50 mL/min. The pan was sealed and transferred to the heating chamber to equilibrate for 2hrs. An empty pan was used as a reference. Rising temperature experiments were conducted at the temperature range from 25 to 300 °C and heating rate of 10° C /min<sup>9</sup>. Data were analyzed using the software Proteus.

**Fourier-transform infrared spectroscopy (FTIR):** Dried PEBE and CBE, 10 mg was encapsulated in 100 mg of KBr pellet so as to organize translucent sample discs. The

powdered sample of every plant specimen was loaded in FTIR spectroscope (BRUKER, FTIR spectrophotometer, Alpha II) with a scan range from 500 to 4000 cm<sup>6</sup>.

**Gas chromatography–mass spectrometry Analysis for identification of compounds (GC-MS):** GC-MS analysis was administered on a Perkin Elmer Turbo-mass coupled with GC-Auto-XL, MS at 70eV using helium as carrier gas<sup>6</sup>.

## Results and Discussion

**Phytochemical Analysis:** The classes of phytochemicals present in the extracts were identified to be oils and fats, alkaloids, carbohydrates, saponin and glycosides in PEBE (phenols, flavonoids and triterpenoids were absent as shown in table 1) and the CBE contained phytochemicals like oils and fats, alkaloids, saponin, polyphenols, cardiac glycoside, tannin and terpenoids as shown in table 2.

**Thermal analysis parameters of extracts:** In this thermograph, it can be observed that with increase in temperature, the substances undergo gradual decomposition, then the change within the mass of the substances occurs with the breaking of chemical bonds at the elevated temperatures. This analytical technique is often used for characterization of plant extracts. The TG curves obtained for *Bauhinia variegata* extracts under N<sub>2</sub> atmosphere (pyrolysis) are presented in fig. 1a and 1b. The extract thermal compartment was divided into three sequential steps, with the primary one associated with loss of loosely bound water due to sample dehydration. In graph's, until 200 °C, PEBE and CBE showed thermal stability with minor variations in mass.

Around 150 - 200 °C, a change in mass% was observed as PEBE – 1.73% and CBE – 4.24% and possibly related to non-oxidative degradation of extracts. Exothermic peaks are representative during the thermal degradation of plant extracts.

**Table 1**  
Qualitative phytochemical analysis of Petroleum ether bark extract of *Bauhinia variegata*

Alkaloids	+	Polyphenols	-
Flavonoids	-	Saponin Glycosides	+
Oils and fats	+	Cardiac glycoside	+
Sterols	-	Terpenoids	-
Saponin	+	Tannin	-
Coumarin	-	Triterpenoids	-

**Table 2**  
Qualitative phytochemical analysis of Chloroform bark extract of *Bauhinia variegata*

Alkaloids	+	Polyphenols	+
Flavonoids	-	Saponin glycosides	-
Carbohydrates	-	Cardiac glycoside	+
Sterols	-	Terpenoids	+
Saponin	+	Tannin	+
Coumarin	-	Triterpenoids	+

Finally, from 350 to 600 °C, the PEBE was thoroughly degraded, leaving 17.96% residual mass. For CBE, from 320 to 600 °C, the extract got fully degraded leaving 21.34% residual mass. This is often mostly due to non-oxidative atmosphere used for thermal analysis. As observed in TGA results of extracts, thermal events like mass losses were within the range of 30–100 °C (Phase I), 100–360 °C (Phase II) and 360–600 °C (Phase III).

DSC (differential scanning calorimetry) is a technique to measure the changes in materials as a function of temperature and time. In fig. 2a and 2b, the schematic DSC curve shows typical thermal effect. The curve shows three transition phases, glass transitions labelled (1), the peak due to crystallization labelled as (2) and eventually the decomposition labelled as (3). Peak area corresponds to the enthalpy involved during the process. For PEBE, the melting temperatures, within the differential scanning calorimetry

(DSC) curve, occurred between 55 and 100°C (peak at 79.4°C) indicating a mix of the extract. For CBE, the melting temperature arose between 50 - 70°C (peak at 51.2°C). The decomposition processes begin above 140°C for PEBE and for CBE and it starts above 110°C.

**Fourier-transform infrared spectroscopy (FTIR):** The data on the peak values and the possible functional groups (obtained by FTIR analysis) present in the bark extracts (prepared in PE, CHL) of *Bauhinia variegata* are presented in fig. 3 and tables 3.

**Petroleum ether (PE) extract:** P.E extract of *Bauhinia variegata* exhibited a characteristic band at 1460 cm<sup>-1</sup> indicating the presence of C-H group, 1734 cm<sup>-1</sup> pair of carbonyls (C=O) group, 2926.34 cm<sup>-1</sup> for C-H stretching and 3437.92 for -OH group.

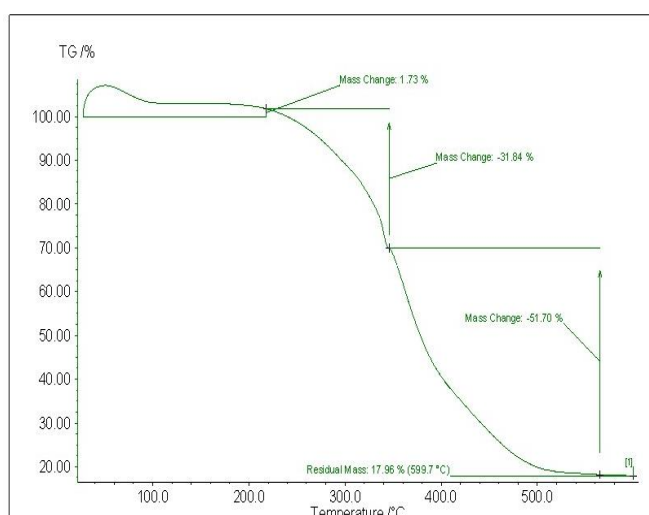
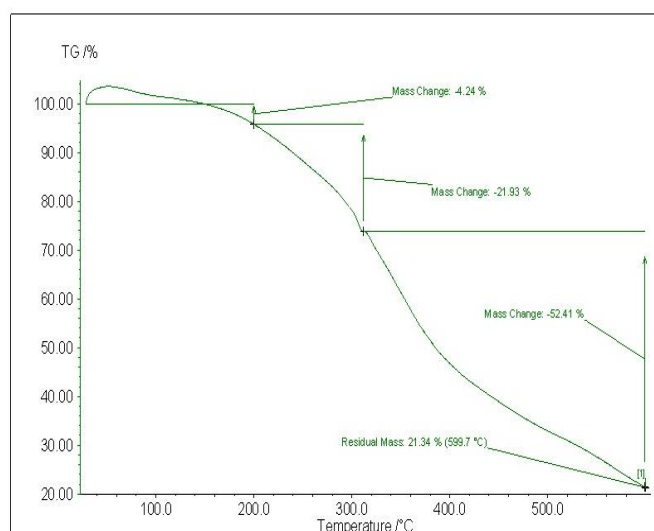


Figure 1: a) TG curves for dried PEBE of *Bauhinia variegata*



b) TG curves for dried CBE of *Bauhinia variegata*

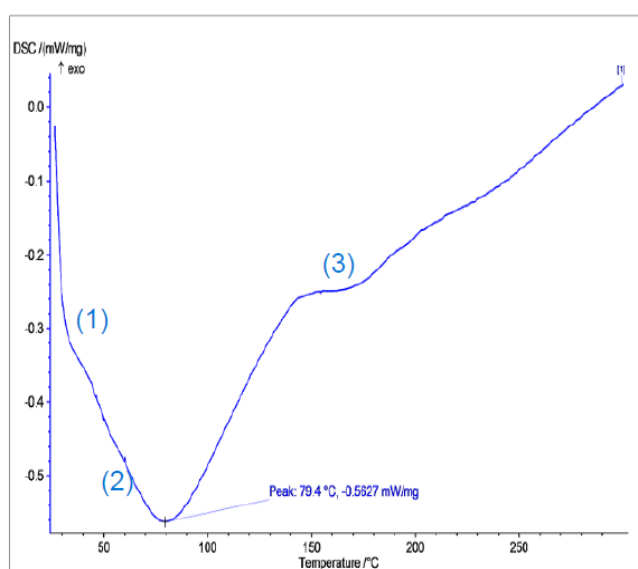
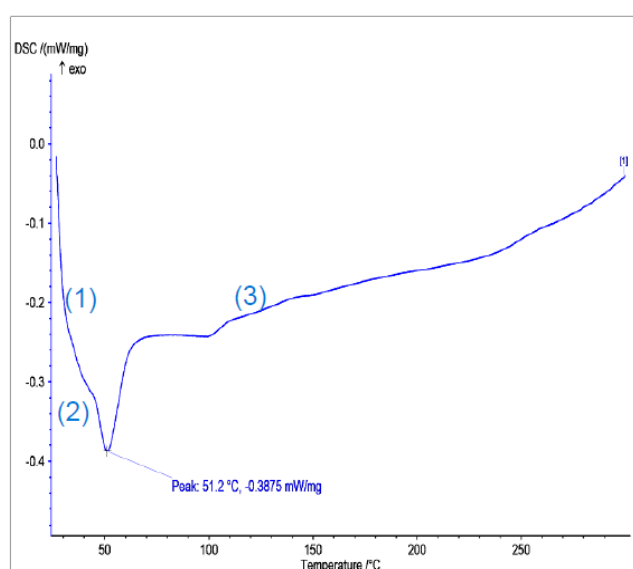


Figure 2: a) DSC curves for dried PEBE of *Bauhinia variegata*



b) DSC curves for dried CBE of *Bauhinia variegata*

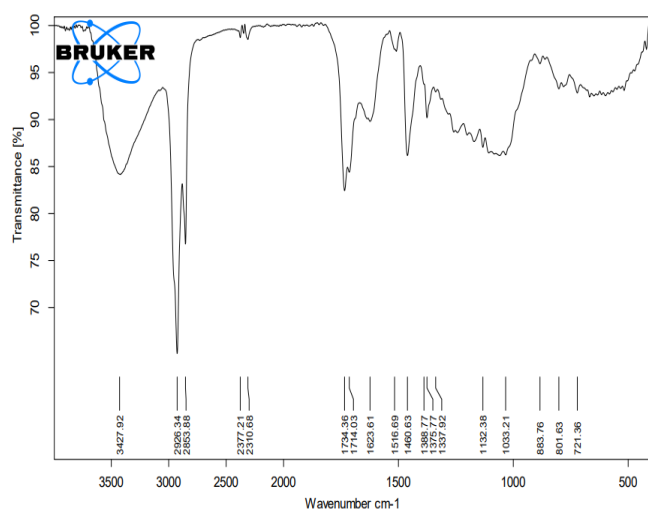
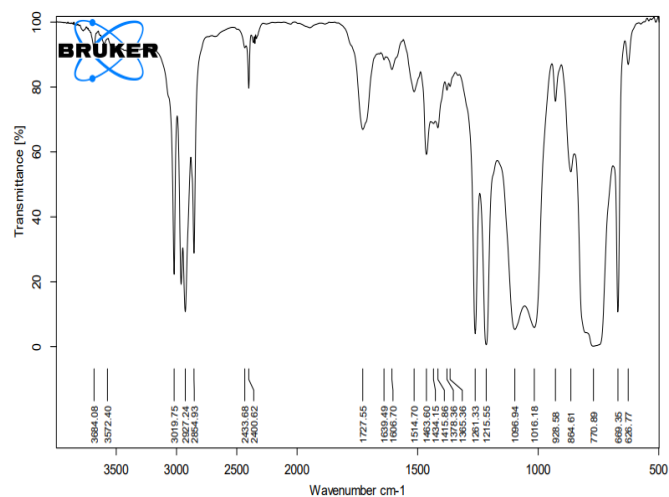
Figure 3: a) FTIR graph of PEBE of *Bauhinia variegata*b) FTIR graph of CBE of *Bauhinia variegata*

Table 3

FTIR spectral peak values and type of groups obtained for the bark extract (in petroleum ether and chloroform bark extract solvents) of *Bauhinia variegata*.

Extracts (Petroleum Ether)	Peak values	Type	Intensity	Extracts Chloroform	Peak values	Type	Intensity
<b>Petroleum Ether</b>	1388.77	C-H bending	m	<b>Chloroform</b>	669.35	C-Br stretch	S
	1460.63	C-H bend	m		770.89	C-H bending	S
	1516.69	C-N=O	S		928.58	C-H stretch	m
	1623.61	C=C group	V		1016.18	C-OH group	S
	1714.03	C=O carbonyl group	S		1096.94	C-OH group	S
	1734.36	C=O carbonyl group	S		1215.55	C=O carbonyl group	S
	2853.88	C-H stretching	S		1261.33	C=O carbonyl group	S
	2926.34	C-H stretching	S		1463.60	C-H stretching	m
<b>Petroleum Ether</b>	3427.92	-OH group	V		1727.55	C=O carbonyl group	S
					2433.68	-NH group	m
					2854.93	-OH group	V
					2927.24	C-H stretching	S
				<b>Chloroform</b>	3019.75	-OH group	V

**Chloroform (CHL) extract:** The characteristic absorption band were exhibited at  $3019.75\text{ cm}^{-1}$  (for OH group),  $2927.24\text{ cm}^{-1}$  (for C-H stretching),  $2854.93\text{ cm}^{-1}$  (for OH group),  $1215.55$  and  $1261.33\text{ cm}^{-1}$ .

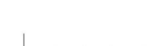
**Gas Chromatography–Mass Spectrometry Analysis:** The GC-MS chromatogram of the PEBE of *Bauhinia variegata* showed the presence of 18 compounds. Identification of the phytochemicals based on the peak area, retention time and molecular formula is shown in table 4. There are eight phytochemicals present in CBE and their molecular formula

and structures are shown in table 5. The compounds at RT 29.65 and 30.35 are reported for the first time from CBE of *Bauhinia variegata*.

### Conclusion

This work showed the application of thermal and FT-IR analysis on a plant derived raw material that can be used to establish parameters on the development of therapeutic products which will help in insuring its quality, safety and efficacy.

**Table 4**  
**Phytocomponents identified in the petroleum ether bark extract (PEBE) of *Bauhinia variegata* by GC-MS**

S.N.	Retention time	Name of compound	Molecular formula	Peak Area	Structure
1.	9.05 min.	Benzene,1,3-bis(1,1-dimethylethyl)	C <sub>14</sub> H <sub>22</sub>	967652.4	
2.	9.43 min.	Trans-2-Undecen-1-ol	C <sub>11</sub> H <sub>22</sub> O	4855124.6	
3.	9.87 min.	Trans-2-undecen-1-ol	C <sub>11</sub> H <sub>22</sub> O	675052.1	
4.	11.52 min.	Oxalic acid, allyl hexadecyl ester	C <sub>21</sub> H <sub>38</sub> O <sub>4</sub>	325052.1	
5.	12.92 min.	1-Iodo-2-methyl undecane	C <sub>12</sub> H <sub>25</sub> I	575052.1	
6.	13.56 min.	Phenol,2,4-bis(1,1-dimethylethyl)	C <sub>14</sub> H <sub>22</sub> O	858468.37	
7.	16.05 min.	Heptadecane, 2,6,10,15-tetramethyl	C <sub>21</sub> H <sub>44</sub>	422998.21	
8.	19.92 min.	Stearic acid hydrazide	C <sub>18</sub> H <sub>38</sub> N <sub>2</sub> O	28781.44	
9.	20.61 min.	Phthalic acid, nonyl tridec-2-yn-1-yl ester	C <sub>30</sub> H <sub>46</sub> O <sub>4</sub>	685803.40	
10.	23.46 min.	n-hexadecenoic acid	C <sub>16</sub> H <sub>32</sub> O <sub>2</sub>	861652.2	
11.	25.04 min.	Oleic acid	C <sub>18</sub> H <sub>34</sub> O <sub>2</sub>	5850124.5	
12.	25.96 min.	Oleic acid	C <sub>18</sub> H <sub>34</sub> O <sub>2</sub>	425052.1	
13.	26.97 min.	2-Methyl-Z-4-tetradecene	C <sub>15</sub> H <sub>30</sub>	375252.2	
14.	27.38 min.	Oleic acid	C <sub>18</sub> H <sub>34</sub> O <sub>2</sub>	672152.0	

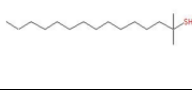
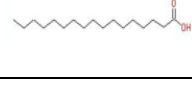
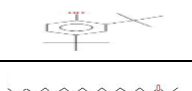
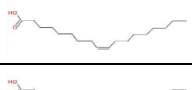
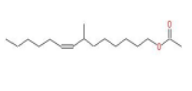
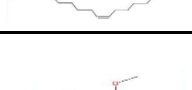
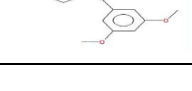
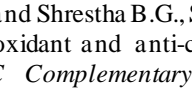
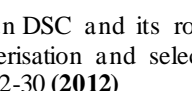
15.	27.64 min.	Erucic acid	$C_{22}H_{42}O_2$	927868.7	
16.	27.96 min.	Tert- Hexadecane thiol	$C_{16}H_{34}S$	521998.21	
17.	29.88 min.	Heptadecanoic acid	$C_{17}H_{34}O_2$	295419.24	
18.	30.76 min.	12- Methyl- E, E- 2,13- octadecadien-1-ol	$C_{19}H_{36}O$	755603.35	

Table 5

Phytochemicals identified in the chloroform bark extract (CBE) of *Bauhinia variegata* by GC-MS

S.N.	Retention time	Name of compound	Molecular formula	Peak Area	Structure
1.	11.04 min.	Phenol,2,4-bis (1,1 -- dimethylethyl)	$C_{14}H_{22}O$	968252.4	
2.	18.82 min.	Hexadecanoic acid, ethyl ester	$C_{18}H_{36}O_2$	7022092.8	
3.	21.96 min.	Oleic acid	$C_{18}H_{34}O_2$	7238706.2	
4.	23.97 min.	Oleic acid	$C_{18}H_{34}O_2$	775052.1	
5.	25.54 min.	7-Methyl-Z-tetradecen-1-ol acetate	$C_{17}H_{32}O_2$	1156491.4	
6.	27.89 min.	Oleic acid	$C_{18}H_{34}O_2$	1442955.4	
7.	29.65 min.	4-(1,1-Dimethylallyl)-9-methoxy-7H-furo (3,2-g) [1] benzopyran-7-one	$C_{17}H_{16}O_4$	4885144.6	
8.	30.35 min.	6-Hydroxy-3(3,5-dimethoxyphenyl)-benzo(b)furan	$C_{16}H_{14}O_4$	39131349.9	

This study also showed that thermal disposal of *Bauhinia variegata* PEBE and CBE results in the release of harmless by products which definitely increase the application of this efficient anti-cancerous drug in pharmaceutical applications where this safe disposal may be used as a commercial claim.

### Acknowledgement

TK did most of the experiments, AD helped in data analysis and PR conceptualized the work. SAIF IIT Mumbai is acknowledged for GC-MS analysis. GIRDA Centre, MS University is acknowledged for TG-DSC analysis and Department of Chemistry, MS University is acknowledged for FTIR analysis.

### References

- Bhandari J., Muhammad B., Thapa P. and Shrestha B.G., Study of phytochemical, anti-microbial, antioxidant and anti-cancer properties of *Allium wallichii*, *BMC Complementary and Alternative Medicine*, **17**, 1-9 (2017)
- Ford J.L. and Mann T.E., Fast-Scan DSC and its role in pharmaceutical physical form characterisation and selection, *Advanced Drug Delivery Reviews*, **64**, 422-30 (2012)
- Gul H. et al, Quantification of biochemical compounds in *Bauhinia Variegata* Linn flower extract and its hepatoprotective effect, *Saudi Journal of Biological Sciences*, **28**, 247-54 (2021)

4. Hago S., Mahrous E.A., Moawad M., Abdel-Wahab S. and Abdel-Sattar E., Evaluation of antidiabetic activity of *Morus nigra* L. and *Bauhinia variegata* L. leaves as Egyptian remedies used for the treatment of diabetes, *Natural Product Research*, **35**, 829-35 (2021)
5. Jamir K., Badithi N., Venumadhav K. and Seshagirao K., Characterization and comparative studies of galactomannans from *Bauhinia vahlii*, *Delonix elata* and *Peltophorum pterocarpum*, *International Journal of Biological Macromolecules*, **1**, 498-506 (2019)
6. Kavitha S., Kannan M.V. and Mani P., Identification of Bioactive Compounds in the leaves extract of *Piper longum* using GCMS, *Research Journal of Pharmacy and Technology*, **13**, 3169-70 (2020)
7. Khazaei S. et al, *In vitro* antiproliferative and apoptosis inducing effect of *Allium atroviolaceum* bulb extract on breast, cervical and liver cancer cells, *Frontiers in Pharmacology*, **8**, 5 (2017)
8. Kolhe R.H., Acharya R. and Shukla V.J., Role of thin-layer chromatography in ascertaining Kashaya Rasa (astringent taste) in medicinal plants on the concept of Samana and Vichitra Pratyayarabdha principles of Ayurveda, *Ayu.*, **35**, 179 (2014)
9. Mishra A., Sharma A.K., Kumar S., Saxena A.K. and Pandey A. K., *Bauhinia variegata* leaf extracts exhibit considerable antibacterial, antioxidant and anticancer activities, *BioMed Research International*, **5**, 10 (2013)
10. Raj Kapoor B., Muruges N. and Rama Krishna D., Cytotoxic activity of a flavanone from the stem of *Bauhinia variegata* Linn. *Natural Product Research*, 2009, **23**, 1384-9 (2009)
11. Sharma N. et al, Isolation of phytochemicals from *Bauhinia variegata* l. Bark and their *in vitro* antioxidant and cytotoxic potential, *Antioxidants*, **8**, 492 (2019)
12. Sousa R., Figueirinha A., Batista M.T. and Pina M.E., Formulation Effects in the Antioxidant Activity of Extract from the Leaves of *Cymbopogon citratus* (DC) Stapf, *Molecules*, **26**, 4518, (2021).

(Received 09<sup>th</sup> November 2021, accepted 10<sup>th</sup> January 2022)

# Exploiting Rhizobium for Cadmium Sulphide Nanoparticle Synthesis: Heterologous Expression of an *Escherichia coli* DH10B Enzyme, YbdK [EC: 6.3.2.2] in *Sinorhizobium fredii* NGR234

Akash Dave , Tanvi Khanna  and Pushpa Robin\* 

Department of Biochemistry, Faculty of Science, The Maharaja Sayajirao University of Baroda, Vadodara - 390 002, Gujarat, India.

## Abstract

*Escherichia coli* DH10B has 1.1 kb ybdK gene which is responsible for encoding YbdK enzyme that possess a Gamma glutamyl cysteine synthetase activity. ybdK gene was ligated downstream of a constitutive derepressed lac promoter of a low copy number plasmid vector pBBR1MCS-2, giving rise to a recombinant plasmid pPAT. *Sinorhizobium fredii* NGR234 transformed with pPAT showed an augmented production of glutathione which in turn increased the production of cadmium sulphide nanoparticles to some extent. Also, a heterologous expression of YbdK in *Sinorhizobium fredii* NGR234 improved the oxidation status of bacterial cells which is confirmed by fluorescence microscopy images and fluorometry. Genetically modified (GM) cells stained by DCFDA showed a significant decrease in fluorescence compared to wild type (WT) cells. Physical and chemical properties of the nanoparticles produced by the pPAT transformed *Sinorhizobium fredii* NGR234 differed significantly compared to wild type (WT) *Sinorhizobium fredii* NGR234. Comparative analysis of the nanoparticles by FTIR and SEM analysis revealed the functional groups attached to nanoparticles and average nanoparticle size respectively. Nanoparticles synthesized by genetically modified (GM) bacteria were about 3 times smaller in size compared to those produced by wild type (WT) rhizobium. FTIR analysis revealed an augmented presence of peptide with the nanoparticles produced by GM bacteria compared to those produced by the WT bacteria. XRD data revealed that biosynthesized CdS nanoparticles are face centered crystalline particles which was confirmed by comparing the peaks to standard JCPDS data (JCPDS card no. 10-454).

**Keywords:** *Sinorhizobium fredii* NGR234, YbdK, Glutathione, Heavy metals, Cadmium sulphide, Nano particles, Green synthesis

\*Correspondence: pushparobin@gmail.com; +91 9879120161

(Received: October 6, 2021; accepted: January 19, 2022)

**Citation:** Dave A, Khanna T, Robin P. Exploiting Rhizobium for Cadmium Sulphide Nanoparticle Synthesis: Heterologous Expression of an *Escherichia coli* DH10B Enzyme, YbdK [EC: 6.3.2.2] in *Sinorhizobium fredii* NGR234. *J Pure Appl Microbiol.* 2022;16(1):593-605. doi: 10.22207/JPAM.16.1.59

© The Author(s) 2022. **Open Access.** This article is distributed under the terms of the [Creative Commons Attribution 4.0 International License](https://creativecommons.org/licenses/by/4.0/) which permits unrestricted use, sharing, distribution, and reproduction in any medium, provided you give appropriate credit to the original author(s) and the source, provide a link to the Creative Commons license, and indicate if changes were made.



## Research paper

# Mononuclear copper(II) and binuclear cobalt(II) complexes with halides and tetradentate nitrogen coordinate ligand: Synthesis, structures and bioactivities



Mehul H. Sadhu<sup>a</sup>, Sujit Baran Kumar<sup>a,\*</sup>, Jaswinder Kaur Saini<sup>b</sup>, Sejal S. Purani<sup>c</sup>, Tanvi R. Khanna<sup>c</sup>

<sup>a</sup> Department of Chemistry, Faculty of Science, The Maharaja Sayajirao University of Baroda, Vadodra 390002, India

<sup>b</sup> Department of Microbiology and Biotechnology Centre, Faculty of Science, The Maharaja Sayajirao University of Baroda, Vadodra 390002, India

<sup>c</sup> Department of Biochemistry, Faculty of Science, The Maharaja Sayajirao University of Baroda, Vadodra 390002, India

## ARTICLE INFO

## Article history:

Received 17 March 2017

Received in revised form 13 May 2017

Accepted 2 June 2017

Available online 3 June 2017

## Keywords:

Tripodal ligand

Copper(II) and cobalt(II) complexes

Spectra

Structure

Bioactivities

## ABSTRACT

In this work, we present the synthesis of four mononuclear copper(II) complexes [Cu(bdpab)X]Y and two binuclear cobalt(II) complexes [Co(bdpab)Cl]<sub>2</sub>Y<sub>2</sub> (X = Cl<sup>-</sup>, Br<sup>-</sup>; Y = PF<sub>6</sub><sup>-</sup>, BF<sub>4</sub><sup>-</sup>) with tripodal N<sub>4</sub>-coordinate N-benzyl-N',N'-bis(3,5-dimethyl-1H-pyrazol-1-yl)-2-methyl-1,2-ethylenediamine (bdpab) and the complexes were characterized by elemental analyses, IR spectral data, molar conductivity measurement, EPR and crystal structure determination. Single crystal X-ray diffraction studies indicate that the copper centers in the complexes [Cu(bdpab)Cl]PF<sub>6</sub> and [Cu(bdpab)Br]PF<sub>6</sub> have distorted square pyramidal geometry and complex [Co(bdpab)Cl]<sub>2</sub>(PF<sub>6</sub>)<sub>2</sub> has octahedral geometry and two [Co(bdpab)Cl]<sup>+</sup> units are linked by two (μ-Cl) bridges. Copper(II) complexes form 1D supramolecular chain along c-axis through C-H-π interaction whereas cobalt(II) complex form 1D supramolecular chain along a-axis through π-π interaction. The antimicrobial activity of complexes [Cu(bdpab)Cl]PF<sub>6</sub>, [Cu(bdpab)Br]PF<sub>6</sub> and [Co(bdpab)Cl]<sub>2</sub>(PF<sub>6</sub>)<sub>2</sub> were investigated against gram positive (*Bacillus subtilis*, *Streptococcus aureus*) and gram negative (*Escherichia coli*, *Pseudomonas aeruginosa*) bacterial strains by agar well dilution method and have demonstrated significant antimicrobial activity of the compounds. [Co(bdpab)Cl]<sub>2</sub>(PF<sub>6</sub>)<sub>2</sub> exhibited the best antibacterial activity among all the synthesized complexes. The studies on the interaction of complexes and DNA by agarose gel electrophoresis method revealed that the complexes can effectively cleave the circular plasmid DNA at very low concentrations. The cytotoxic activity of the complexes against A549 lung cancer cells showed that the complexes have better cytotoxic activity than corresponding metal salts and [Cu(bdpab)Br]PF<sub>6</sub> complex has best cytotoxic activity among the synthesized complexes.

© 2017 Elsevier B.V. All rights reserved.

## 1. Introduction

Since the discovery of cis-platin as an anti-cancer agent, design and synthesis of new transition metal compounds and their interaction with DNA have been an important area of research in bioinorganic chemistry for the development of new material as the therapeutic agent [1–4]. It is well known that gene has important role in the biological process and the study of the interaction of DNA with transition metal complexes is important for the development of less toxic, target specific and less side effect of the transition metal containing metallodrug [5–7]. Transition metal complexes are used as bioactive complex because they have different binding ability, coordination numbers and oxidation states etc.

Among the transition metal complexes investigated as therapeutic agent, majority are from copper as it is an essential element for the biological system and has low toxicity [8–16]. Since cobalt is also important elements in the bio system, the interaction of cobalt with DNA has been attracted recently [17,18]. Since the DNA and transition metal interaction depends on the donor atom of the ligand, nitrogen coordinating ligands such as poly-pyridine are used mostly for the synthesis of bioactive transition metal complexes [19,20]. Many copper(II) and cobalt(II) complexes with tripodal ligands have been investigated for their anticancer properties [21–23]. There are few reports on the bioactivities on the model complexes of bleomycin with imidazole, pyrimidinyl amino and amino donor groups of ligands [24–26]. Since there are some similarities between the metal binding of model complexes and metal complexes with tripodal pyrazole-based N<sub>4</sub>-tetradentate ligands, we are interested to study the bioactivities of the copper(II) and cobalt(II) complexes with this pyrazolyl containing ligand.

\* Corresponding author.

E-mail address: [sujit\\_baran@yahoo.com](mailto:sujit_baran@yahoo.com) (S.B. Kumar).